

### Probe Report

**Title:** Discovery, SAR and Biological Evaluation of Aryl-thiazol-piperidines as SMN Modulators

**Authors:** Jingbo Xiao<sup>a</sup>, Juan J. Marugan<sup>a\*</sup>, Wei Zheng<sup>a</sup>, Steve Titus<sup>a</sup>, Noel Southall<sup>a</sup>, Jonathan J. Cherry<sup>b</sup>, Matthew Evans<sup>b</sup>, Elliot J. Androphy<sup>b</sup>, and Christopher P. Austin<sup>a</sup>

<sup>a</sup> NIH Chemical Genomics Center, National Human Genome Research Institute, National Institutes of Health, 9800 Medical Center Drive, Rockville, Maryland 20850.

<sup>b</sup> Department of Medicine, University of Massachusetts Medical School, 364 Plantation Street, LRB 328, Worcester, Massachusetts 01605.

\* To whom correspondence should be addressed: NIH Center for Translational Therapeutics, NIH Chemical Genomics Center, National Human Genome Research Institute, National Institutes of Health, 9800 Medical Center Drive, Bldg B, Rockville, MD 20850. Phone: 301-217-9198. Fax: 301-217-5736. Email: [maruganj@mail.nih.gov](mailto:maruganj@mail.nih.gov)

Assigned Assay Grant #: MH084179-01

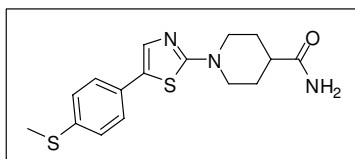
Screening Center Name & PI: NIH Chemical Genomics Center, Christopher Austin

Chemistry Center Name & PI: NIH Chemical Genomics Center, Christopher Austin

Assay Submitter & Institution: Elliot Androphy, University of Massachusetts Medical School

PubChem Summary Bioassay Identifier (AID): 1474

### Probe Structure & Characteristics:



ML200

PubChem CID: 46907676/ML200

Internal ID: NCGC00187898-01

IUPAC Name: 1-(5-(4-(methylthio)phenyl)thiazol-2-yl)piperidine-4-carboxamide

Chemical Formula: C<sub>16</sub>H<sub>19</sub>N<sub>3</sub>OS<sub>2</sub>

Exact Mass: 333.0970

CID/ML#	Target Name	IC50/EC50 (nM) [SID, AID]	Anti-target Name(s)	IC50/EC50 (μM) [SID, AID]	Fold Selective	Secondary Assay(s) Name: IC50/EC50 (nM) [SID, AID]
46907676/ML200	SMN2 Protein expression	31 nM [99367992, 488832]	SMN1 protein expression	0.972 μM [99367992, 488821]	31 fold	Western Blot of SMN protein in patient fibroblasts: 37 nM [99367992, 1474]
			Luciferase inhibition	40.08 μM [99367992, 488838]	> 1000-fold	

### Recommendations for scientific use of the probe:

Spinal Muscular Atrophy (SMA) is an autosomal recessive disorder affecting the selective degeneration of survival motor neuron (SMN) in the spinal cord due to the deletion or mutations of the survival motor neuron gene 1 (*SMN1*). However, the human genome includes a second nearly identical gene called *SMN2* which functionally differs from *SMN1* by a critical nucleotide C to T transition residing in exon 7. Although *SMN2* is able to produce a small portion of full length SMN protein, the majority of *SMN2* RNAs undergo alternative splicing and produce truncated, proteolytically unstable SMN variants that are not able to replace the function of full length SMN protein. Therefore, increasing overall SMN production through up-regulation of *SMN2* expression or through the variation of splicing rate has been postulated to be one of the potential therapeutic strategies for SMA. In this report, we detail the discovery of a series of arylpiperidines as novel modulators of SMN protein production from a qHTS campaign of the 210,386-compound NIH Molecular Libraries of Small Molecule Repository. Systematic hit-to-lead medicinal chemistry efforts on this series dramatically improved both potency (up to 100 fold) and efficacy (up to 2 fold) of the series. Several lead compounds were identified as having very high potency, and a capacity to increase 3 to 7 fold induction of SMN promoter in the reporter assay including analogs **8i** ( $AC_{50} = 77\text{nM}$ , rate of induction = 710%), **8m** (CID: 46907676/ML200, current updated probe compound,  $AC_{50} = 31\text{nM}$ , rate of induction = 576%), and **9a** ( $AC_{50} = 12\text{nM}$ , rate of induction = 326%). Furthermore, the activity of probe compound **8m** was confirmed by western blot analysis and gem count assay using SMA patient fibroblasts at low nanomolar range (37nM). The structure property relationships (SPR) including microsomal stability, cell permeability and full time oral dosing *in vivo* pharmacokinetic studies were also investigated to address ADME properties. We anticipate that the updated probe compound **8m** may serve as a useful lead for exploring the therapeutic benefits of SMN protein induction in SMA animal models, and ultimately in human clinical trials.





## 1 Introduction

Spinal Muscular Atrophy (SMA), an inherited autosomal neurodegenerative disease, is the leading genetic disorder affecting infant mortality.<sup>i</sup> SMA is a relatively common "rare disease"; approximately 1 in 6,000 born babies are affected, and about 1 in 40 individuals are genetic carriers.<sup>ii</sup> Clinically, there are five types of SMA (SMA Type 0, I, II, III, and IV), and the determination of the type of SMA is based upon the physical milestones achieved. Usually children with the most severe form of the disease (Type 1; Werdnig-Hoffmann disease) die before the age of two years in the absence of supportive respiratory care.<sup>iii</sup> In fact, **SMA** is the **number one** genetic **killer** of children under the age of two, and many of those children who make it through infancy will be confined to wheelchairs for their entire lives. There is currently no cure or effective disease modifying therapy for SMA.

SMA is caused by a deficiency of an essential protein (SMN, survival motor neuron) containing 294 amino acids due to homozygous mutations or deletion of the survival motor neuron 1, telomeric (*SMN1*) gene which is located on chromosome 5q13.<sup>iv</sup> The SMN protein is ubiquitously expressed and its level of expression is tissue dependent,<sup>v</sup> but its significant reduction leads to rapid degeneration and death of alpha-motor neurons in the anterior horn of the spinal cord. Studies of the correlation between SMA severity and the amount of survival motor neuron (SMN) protein have shown an inverse relationship.<sup>vi</sup> From the functional point of view, SMN associates with proteins Gemin 2, Gemin 3 and Gemin 4, forming a large complex that plays a role in snRNP assembly, pre-mRNA splicing and transcription.<sup>vii</sup> Humans possess an additional paralogous gene, survival motor neuron 2, a centromeric (*SMN2*) gene whose sequence only functionally differs at a single nucleotide from the *SMN1* gene (C-T).<sup>viii</sup> Though full length 38 kDa SMN protein can be produced from the transcription of both *SMN1* and *SMN2* homolog genes, variation of a single nucleotide in exon 7 has a large impact on gene splicing. The vast majority of the pre-mRNA transcripts from *SMN1* gene produces full-length mRNA with nine exons encoding full-length of SMN protein, while the C- to T- transition at position six in exon 7 of *SMN2* causes mostly alternative pre-mRNA splicing lacking exon 7, which results in the production of a truncated SMN protein (termed as SMN $\Delta$ 7) as the main product; is the production of full length SMN from *SMN2* gene is less than 20% of all splicing variants. SMN $\Delta$ 7 protein is functional, but it has a reduced ability for self-oligomerization, leading to protein instability and rapid degradation.<sup>ix</sup> *SMN2* has been a target for SMA therapy, since all human SMA patients maintain one or more copies of *SMN2* gene, and there is a striking correlation between SMA type and severity and *SMN2* gene copy numbers.<sup>x</sup>

Though there are several alternative SMA therapeutic strategies under investigation, such as gene therapy,<sup>xi</sup> antisense oligonucleotides (ATO) therapy<sup>xii</sup> and stem cells therapy<sup>xiii</sup>, increasing the production of SMN protein by modulation of the *SMN2* expression induced by small molecules has been proposed as a promising potential therapeutic strategy for SMA. Over the past several years, a number of small molecule classes have been identified as increasing SMN transcript and/or protein levels in SMA patient-derived cell lines through a variety of mechanisms.<sup>xiv</sup> Tsai et al reported that sodium butyrate, a classical

histone deacetylase (HDAC) inhibitor, effectively increased the amount of exon 7-containing SMN protein in SMA lymphoid cell lines. *In vivo*, sodium butyrate treatment of SMA-like mice resulted in increased expression of SMN protein in motor neurons of the spinal cord, and resulted in significant improvement of SMA clinical symptoms.<sup>xv</sup> Sodium 4-phenylbutyrate (PBA), an analog of sodium butyrate, was also found to increase SMN expression *in vitro*. PBA has a much longer half life time (1.5 hours) in human serum compared with sodium butyrate (6 minutes), which suggested that PBA, owing also to its favorable pharmacological properties, could be a better candidate for the treatment of SMA.<sup>xvi</sup> The FDA approved antineoplastic drug, hydroxyurea, was recently reported as a candidate SMA therapeutic able to modestly increase SMN production but having a strong safety profile, high pediatric bioavailability, and known capacity for gene upregulation.<sup>xvii</sup> Other bioactive agents,<sup>xviii</sup> such as valproic acid,<sup>xix</sup> aclarubicin (aclacinomycin A),<sup>xx</sup> tobramycin and amikacin<sup>xxi</sup>, Trichostatin A (TSA),<sup>xxii</sup> suberoylanilide hydroxamic acid (SAHA),<sup>xxiii</sup> EIPA [5-(*N*-ethyl-*N*-isopropyl)-amiloride],<sup>xxiv</sup> LBH589,<sup>xxv</sup> and (*E*)-Resveratrol<sup>xxvi</sup> have been shown in cell based assays to increase levels of exon 7-containing SMN transcript and/or overall SMN protein.

However, all of those repurposed agents have significant liabilities that include gastrointestinal bleeding, short half-life in human serum, high toxicity and lack of target specificity. Lunn et al. identified indoprofen as having an effect on full length *SMN2* expression in a cell-based reporter assay, which up-regulated the SMN protein through a cyclooxygenase-independent mechanism, but it was not potent (> 1  $\mu$ M) and increased protein expression by only 13% (p-value < 0.0139).<sup>xxvii</sup> Recently, a tetracycline compound, PTK-SMA1, was found to promote *SMN2* exon 7 splicing. However, this compound does not penetrate the blood-brain-barrier or increase SMN protein concentration in the central nervous system.<sup>xxviii</sup> Another previous high-throughput screen identified two novel chemical series that can modulate reporter activity in a cell-based *SMN2* promoter assay.<sup>xxix</sup> The most promising, identified as D156844, appears to target DcpS, which modulates SMN protein levels by stabilizing the *SMN2* mRNA transcript.<sup>xxx</sup> Oral administration of D156844 increased the mean lifespan of *SMN $\Delta$ 7* SMA mice by approximately 21-30% when given prior to motor neuron loss.<sup>xxxi</sup> After the sponsor, deCode, removed the compound's off-target activity, reduced its toxicity, and improved its potency and brain permeability, the company produced the current clinical candidate D157495.<sup>xxxii</sup> However, it has not been shown whether this series of molecules acts specifically on *SMN2* mRNA transcript stability.<sup>xxxiii</sup>

We are particularly interested in identifying small molecules that can increase the level of full length SMN protein for therapeutic intervention. This can be achieved by modulating splicing, increasing the level of transcript produced, or stabilizing the SMN protein. In order to achieve this goal, we performed a high-throughput screen in a cell-based reported assay of *SMN2* expression, for the purposes of discovering novel compound classes with novel mechanisms. We previously disclosed two compounds, CID 6404603 (**1**) and CID 990823 (**2**), which might be useful in this regard. The present report updates work on this second series and reports on an improved probe molecule.

## 2 Materials and Methods

### Chemistry general methods

Unless otherwise stated, all reactions were carried out under an atmosphere of dry argon or nitrogen in dried glassware. Indicated reaction temperatures refer to those of the reaction bath, while room temperature (rt) is noted as 25 °C. All solvents were of anhydrous quality purchased from Aldrich Chemical Co. and used as received. Commercially available starting materials and reagents were purchased from Aldrich, TCI and Acros and were used as received. Analytical thin layer chromatography (TLC) was performed with Sigma Aldrich TLC plates (5 × 20 cm, 60 Å, 250 µm). Visualization was accomplished by irradiation under a 254 nm UV lamp. Chromatography on silica gel was performed using forced flow (liquid) of the indicated solvent system on Biotage KPSil pre-packed cartridges and using the Biotage SP-1 automated chromatography system. <sup>1</sup>H NMR spectra were recorded on a Varian Inova 400 MHz spectrometer. Chemical shifts are reported in ppm with the solvent resonance as the internal standard (CDCl<sub>3</sub> 7.27 ppm, DMSO-*d*<sub>6</sub> 2.49 ppm, for <sup>1</sup>H NMR). Data are reported as follows: chemical shift, multiplicity (s = singlet, d = doublet, t = triplet, q = quartet, sep = septet, quin = quintet, br = broad, m = multiplet), coupling constants, and number of protons. Low resolution mass spectra (electrospray ionization) were acquired on an Agilent Technologies 6130 quadrupole spectrometer coupled to an Agilent Technologies 1200 series HPLC. The HPLC retention time were recorded through standard gradient 4% to 100% acetonitrile (0.05% TFA) over 7 minutes using Luna C<sub>18</sub> 3 micron 3 × 75 mm column with a flow rate of 0.800 mL/min. High resolution mass spectral data was collected in-house using an Agilent 6210 time-of-flight mass spectrometer, also coupled to an Agilent Technologies 1200 series HPLC system.

### Biology reagents

All cell culture reagents were purchased from Invitrogen. The white solid bottom 1536 well, tissue culture treated plates came from Greiner. The OneGlo luciferase detection reagent was from Promega. The luciferase enzyme and buffers came from Sigma Aldrich. The 4f11 and 4B7 SMN antibodies were provided to JJC, ME, and EJA as a generous gift from Christian Losron (University of Missouri). Goat anti-mouse HRP-conjugated secondary and α-tubulin antibodies (DM1α) were supplied by Sigma.

## **2.1 Assays**

### 2.1.1 Primary screen

This screen utilizes a luciferase reporter gene assay, combining the promoter and splicing based cassettes in tandem with the major portion of the native *SMN2* cDNA, which was stably transfected into HEK293 cells. Compounds that increase the *SMN2*-luciferase reporter fusion signal presumably enhance expression of the functional *SMN2* splice variant – the full length protein including exon-7.

#### *Assay protocol:*

Passaging media contained DMEM w/ glutamax (+phenol red) 10% FCS, 1x pen/strep, 200 µg/ml hygro, 1x sodium pyruvate. Assay media contained DMEM w/ glutamax (-phenol red) 10% FCS, 1x pen strep, 1x pyruvate.

Sequence, Parameter, Value, Description

(1) Cells, 5 µL, 2000 cells/well, 1536 TC treated White solid bottom plate;

- (2) Time, 10-12 hours, 37 °C, 5% CO<sub>2</sub>;
- (3) Compound, 23 nL, MLSMR Library;
- (4) Control Compound, 23 nL, Sodium butyrate standard 4.5mM (final) conc.;
- (5) Time, 30-36 hours, 37 °C, 5% CO<sub>2</sub>;
- (6) Reagent, 3 µl, OneGlo (TM) from Promega;
- (7) Time, 5-15 minutes, Room temperature;
- (8) Detector, Viewlux: luminescent read, 60 second integration, high speed 2x binning.

210,386 compounds were screened in 1229 1536-well plates over 5 days on the robotic system (1,887,744 wells). Signal-to-background averaged 9-fold and Z' was 0.53. There were many potent hits in this screen; however, many of these compounds were known to potentially inhibit luciferase.

### 2.1.2 SMN2-luciferase reporter assay

HEK-293 cells stably expressing the *SMN1* or *SMN2* reporter construct were maintained and passaged in complete DMEM media containing phenol red, glutamax, sodium pyruvate, 10 % FCS, 1x pen/strep, and 200 µg/mL hygromycin. Cells were assayed in the same media lacking only hygromycin. For the HTS, cells were plated at a density of 2000 cells/well in 5 µL of media and were allowed to adhere overnight at 37 °C in 90% humidity with 5% CO<sub>2</sub>. After incubation, cells received 23 nL of compound library (in 100% DMSO) by pintool addition (Kalypsys). The final concentration of DMSO was 0.46%. The screen was conducted in a 7 point qHTS titration with a final concentration of 50 µM to 25 nM. The positive control compound used was sodium butyrate (4.5 mM final concentration) and the negative control compound was DMSO. Plates were incubated in the presence of compounds for 30 to 36 hours in the humidified incubator. After incubation, cells were treated with 3 µL of OneGlo luciferase detection reagent and incubated at room temperature for 5 to 15 minutes. Luminescence was detected on a Viewlux CCD based instrument (Perkin Elmer) with settings of 60 second integration and high speed 2x binning. Data was normalized against sodium butyrate (100%) and DMSO (0%) treatments.

### 2.1.3 Firefly luciferase enzyme assay

The firefly luciferase enzyme was assayed at 5 nM in buffer consisting of 50 mM Tris-acetate pH 7.6, 10 mM Mg acetate 0.05% BSA, 0.01% Tween. Enzyme (2.5 µL/well) was dispensed in a white solid bottom 1536 well plate and compounds (23 nL) were added using a pintool. Plates were incubated at room temperature for 5 minutes followed by the addition of 2.5 µL of OneGlo luciferase detection reagent. Luminescence was detected in the Viewlux with a 1 second integration time, no binning and medium camera sensitivity.

### 2.1.4 SMN Protein Detection

For detection of SMN protein in patient fibroblasts, 8,000 cells per cm<sup>2</sup> were plated 24 hours prior to drug addition. Fresh media and compound were added every 24 hours. After 72 hours, cells were harvested, washed with cold PBS, and lysed as above. We have determined that 10 µg total proteins per lane are within the linear range for immunoblot detection of SMN and α-tubulin. Western blots were probed for SMN with the 4f11 mouse monoclonal antibody and α-tubulin. Quantification of protein was performed with Fujifilm LAS-4000 Multifunctional Imaging System. The signal intensity was measured for each

band on an immunoblot, normalized to the loading control, and the fold increase was determined in relation to the appropriate DMSO treated control. Gem counts were performed as previously described.

### 2.1.5 Caco-2 Permeability and Microsomal Stability

Analytical signal was optimized for each compound by ESI positive or negative ionization mode. A MS2 SIM scan was used to optimize the precursor ion and a product ion analysis was used to identify the best fragment for analysis and to optimize the collision energy. Samples were analyzed by LC/MS/MS using either an Agilent 6410 mass spectrometer coupled with an Agilent 1200 HPLC and a CTC PAL chilled autosampler, all controlled by MassHunter software (Agilent), or an ABI2000 mass spectrometer coupled with an Agilent 1100 HPLC and a CTC PAL chilled autosampler, all controlled by Analyst software (ABI). After separation on a C18 reverse phase HPLC column (Agilent, Waters, or equivalent) using an acetonitrile-water gradient system, peaks were analyzed by mass spectrometry (MS) using ESI ionization in MRM mode.

CaCo-2 cells grown in tissue culture flasks are trypsinized, suspended in medium, and the suspensions were applied to wells of a collagen-coated BioCoat Cell Environment in 24-well format (BD Biosciences) at 24,500 cells per well. The cells are allowed to grow and differentiate for three weeks, feeding at 2-day intervals.

For Apical to Basolateral (A->B) permeability, the test agent is added to the apical (A) side and amount of permeation is determined on the basolateral (B) side; for Basolateral to Apical (B>A) permeability, the test agent is added to the B side and the amount of permeation is determine on the A side. The A-side buffer contains 100 µM Lucifer yellow dye, in Transport Buffer (1.98 g/L glucose in 10 mM HEPES, 1x Hank's Balanced Salt Solution) pH 6.5, and the B-side buffer is Transport Buffer, pH 7.4. CaCo-2 cells are incubated with these buffers for 2 h., and the receiver side buffer is removed for analysis by LC/MS/MS. To verify that CaCo-2 cell monolayers are properly formed, aliquots of the cell buffers are analyzed by fluorescence to determine the transport of the impermeable dye Lucifer Yellow.

$$P_{app} = \frac{dQ/dt}{C_0 A}$$

Data are expressed as permeability (Papp):

where dQ/dt is the rate of permeation, C0 is the initial concentration of test agent, and A is the area of the monolayer. In bidirectional permeability studies, the asymmetry index (AI) or efflux ratio is also calculated:

$$AI = \frac{P_{app}(B \rightarrow A)}{P_{app}(A \rightarrow B)}$$

An AI > 1 indicates a potential substrate for PGP or other active transport.

For microsomal stability testing, the test agent is incubated in duplicate with microsomes at 37 °C. The reaction contains microsomal protein in 100 mM potassium phosphate, 2 mM NADPH, 3 mM MgCl<sub>2</sub>, pH 7.4. A control is run for each test agent omitting NADPH to detect NADPH-free degradation. At indicated times, an aliquot is removed from each experimental and control reaction and mixed with an



equal volume of ice-cold Stop Solution (0.3% acetic acid in acetonitrile containing haloperidol, diclofenac, or other internal standard). Stopped reactions are incubated at least ten minutes at -20 °C, and an additional volume of water is added. The samples are centrifuged to remove precipitated protein, and the supernatants are analyzed by LC/MS/MS to quantitate the remaining parent. Data are reported as % remaining by dividing by the time zero concentration value.

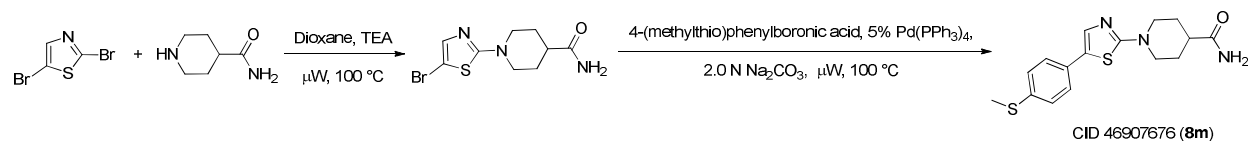
### 2.1.6 Single Oral Dose Pharmacokinetic Study in Male Swiss Albino Mice

Compound was dosed orally to mice, and plasma and brain concentrations were determined pre-dose and at 0, 5, 15, 30, 60, 120, 240, 480, 720, and 1440 minutes, with 4 animals per time point. Male Swiss Albino mice used in this experiment were procured from National Institute of Nutrition (NIN), Hyderabad, India. Animals were acclimatized for three days in an animal holding room. Test article CID was dissolved in DMA, TEG and Water for Injection in the ratio of 20:40:40, and vortexed. Compound was administered orally using stainless steel gavage needle at a dose level of 30 mg/kg at dose volume of 10 mL/kg. After dosing of each animal, animals were observed for any abnormal behavioral signs exhibited after drug administration.

Each mouse was anesthetized using Isoflurane. Blood was collected through a capillary, guided in retro-orbital plexus. The blood samples were collected in prelabeled Heparin coated tubes (BD, cat. No. 365965). 0.3 mL of blood was collected from each mouse at their respective time points. After collection of blood samples at each time point, the blood samples were stored on wet ice prior to centrifugation. Blood samples were centrifuged within 15 minutes to separate plasma at 5000 rpm, 4°C for 10 minutes. The plasma was separated and transferred to pre labeled tubes and promptly frozen at -80 ± 10 °C until bioanalysis. Immediately after blood withdrawal for PK estimation, *in situ* whole body perfusion was performed using chilled saline. The chest and abdomen of the mouse was exposed, the inferior venacava was cut and Intra-cardiac perfusion was performed through an insertion in the left ventricle. Perfusion for each mouse was followed by decapitation for brain collection. The skin over the cranium was incised and deflected. The head was flexed and a cut was made through the muscles and the spinal cord at the junction of the foramen magnum and atlas vertebra. A circumferential incision was carefully made in the cranium using a pair of small scissors. The roof of the cranium was lifted off to expose the meninges and brain. The meninges were removed carefully. Then holding the head with the nose pointing upward, the anterior part of the brain was lifted to separate the brain. Separated brain was immediately weighed and frozen at -80 ± 10 °C until homogenization. PK parameters are calculated for mean concentration by the non-compartmental model, trapezoid rule (linear interpolation method) using WinNonlin Software Version 4.1.

## 2.2 Probe Chemical Characterization

### 2.2.0 Synthetic route of the probe (CID 46907676/ML200, **8m**)



### 2.2.1 Structural verification information of probe (CID 46907676/ML200, **8m**)

1-(5-(4-(methylthio)phenyl)thiazol-2-yl)piperidine-4-carboxamide (CID 46907676/ML200, **8m**). <sup>1</sup>H NMR (400 MHz, *DMSO-d*<sub>6</sub>) δ ppm 7.58 (s, 1 H), 7.37 - 7.45 (m, 2 H), 7.32 (br. s., 1 H), 7.21 - 7.29 (m, 2 H), 6.83 (br. s., 1 H), 3.91 (dt, *J*=12.9, 3.0 Hz, 2 H), 3.09 (td, *J*=12.5, 2.8 Hz, 2 H), 2.48 (s, 3 H), 2.37 (tt, *J*=11.6, 4.0 Hz, 1 H), 1.81 (dd, *J*=13.5, 3.5 Hz, 2 H), 1.54 - 1.67 (m, 2 H); <sup>19</sup>F NMR (376 MHz, *DMSO-d*<sub>6</sub>) δ ppm -74.56 (s);

LC/MS (Agilent system) Retention time *t*<sub>1</sub> (long) = 4.050 min; *m/z* 334.1 [M+H<sup>+</sup>];

HRMS (ESI) *m/z* calcd for C<sub>16</sub>H<sub>20</sub>N<sub>3</sub>OS<sub>2</sub> [M+H<sup>+</sup>] 334.1048, found 334.1048;

Purity: UV<sub>220</sub> > 95%, UV<sub>254</sub> > 95%;

Column: 3 x 75 mm Luna C<sub>18</sub>, 3 micron;

Run time: 4.050 min (long);

Gradient: 4 % to 100 % over 7 min;

Mobile phase: acetonitrile (0.05 % TFA), water (0.05 % TFA);

Flow rate: 0.800 mL;

Temperature: 50 °C;

UV wavelength: 220 nm, 254 nm.

### 2.2.2 Summary of probe properties

CID 46907676/ML200 is soluble at 10 mM concentration in DMSO. The compound is not fluorescent at blue excitation wavelengths (~340 nm)

Solubility (PBS, pH 7.4) at room temperature (23 °C): 2.1 μM

Experimental Log D: 2.41

Stability in phosphate buffered saline (PBS) at room temperature (23 °C): ongoing, will update when the data is available

PubChem CID: 46907676; ML#: 200; SID: 99367988

Molecular Weight: 333.10

Molecular Formula: C<sub>16</sub>H<sub>19</sub>N<sub>3</sub>OS<sub>2</sub>

ClogP: 2.1745

H-Bond Donor: 1.0

H-Bond Acceptor: 2.0

Rotatable Bond Count: 4.0

Exact Mass: 333.0970

Topological Polar Surface Area: 59.22

IUPAC Name: 1-(5-(4-(methylthio)phenyl)thiazol-2-yl)piperidine-4-carboxamide.

### 2.2.3 Canonical SMILES:

CSC1=CC=C(C=C1)C2=CN=C(S2)N3CCCC(CC3)C(N)=O

2.2.2 Provide MLS# that verifies the submission of probe molecules and five related samples that were submitted to the SMR collection:

MLS000698854 (previous probe)

MLS002391463

MLS000710046

MLS002391471

MLS002391472

MLS002391474

## 2.3 Probe Preparation

### 2.3.1 Synthesis of the probe and its analogs

Figure 1 shows the initial SAR strategy designed for this series, including evaluation of aromatic substitutions, the geometry and substituents of the thiazole core, as well as the modification of the piperidine functional group.

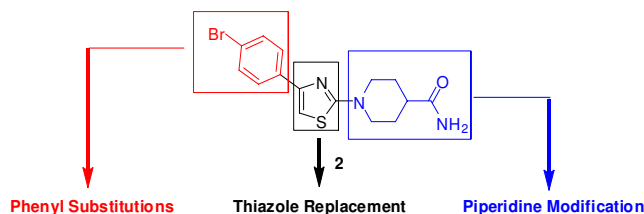


**Figure 1.** SAR strategy.

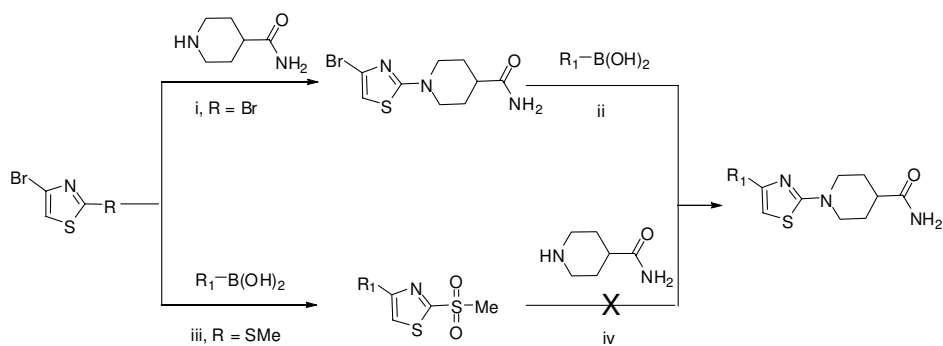
We developed convergent synthetic routes toward the original 2<sup>nd</sup> probe compound CID 990823 (**2**) and its 4-arylthiazolyl piperidine analogs (Scheme 1). The top route was designed for preparing the analogs with the modification of substitutions on the phenyl ring. Starting with 2,4-dibromothiazole, selective amination occurred at the 2-position of the thiazole ring to give the key building block 1-(4-bromothiazol-2-yl)piperidine-4-carboxamide.<sup>xxxiv</sup> Then, a mixture of an arylboronic acid or its corresponding pinacol ester and 1-(4-bromothiazol-2-yl)piperidine-4-carboxamide was irradiated under microwaves to induce a Suzuki type of cross-coupling reaction<sup>xxxv</sup> using tetrakis(triphenylphosphine)palladium(0) as a catalyst to furnish the final 4-arylthiazolyl piperidine analogs. Alternatively, a Suzuki coupling at 4-position of the 2-methylthio-4-bromothiazole, followed by MCPBA oxidation of methylthioyl group to methylsulfonyl moiety to give another building block 4-aryl-2-(methylsulfonyl)thiazole. However, the displacement of methylsulfonyl group of 4-aryl-2-(methylsulfonyl)thiazole with the secondary amine proved to be very difficult. Thus, all of the analogs in this article were prepared through the top route (amination-Suzuki). This synthetic route was straightforward and provided for rapid SAR studies.

In a similar reaction fashion, if the starting material, 2,4-dibromothiazole was replaced by 2,5-dibromothiazole,<sup>xxxvi</sup> 2,5-dibromothiadiazole,<sup>xxxvii</sup> 5-bromo-2-chloropyrimidine,<sup>xxxviii</sup> 2,4-dichloropyrimidine,<sup>xxxix</sup> 4,6-dichloropyrimidine,<sup>xl</sup> or 2,4-dichloro-1,3,5-triazine,<sup>xli</sup> this would echo the corresponding modifications at the thiazole core template as detailed in Scheme 2. It was also interesting to note that the replacement of thiazole with imidazole or *N*-methylimidazole was unsuccessful under the same reaction conditions. All aminated building blocks underwent the same type of Suzuki coupling procedure to give the desired final analogs.

A similar procedure was utilized to further explore the piperidine-4-carboxamide moiety modification (Scheme 3). In the process of typical amination-Suzuki steps, piperidine-4-carboxamide can be successfully switched to ethyl piperidine-4-carboxylate, piperazine, *tert*-butyl piperidin-4-ylcarbamate, piperidine-4-carbonitrile, 1-(piperidin-4-yl)ethanone as well as 4-(1H-imidazol-2-yl)piperidine, but not piperazine-1-carboxamide. Within our SAR studies, we were interested in examining several related substituted amide derivatives. Saponification of the ethyl ester afforded the appropriated acid, which can be readily coupled with amines to provide the final substituted amide modification analogs. We were also

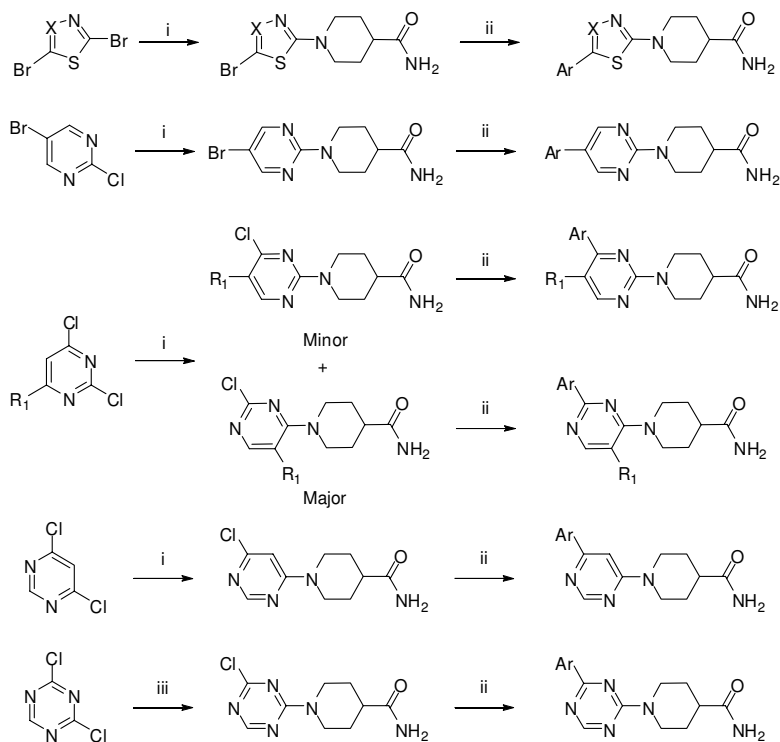
interested in replacing the piperidine with *N*-substituted piperazines. To access these derivatives, the free secondary amine on the piperazine ring can be easily converted into corresponding urea, amides, and sulfonylamides. Finally, a reversed amide bond analog and a tetrazole analog were successfully synthesized as detailed in the Scheme 3, respectively. Most of the final compounds were purified by preparative scale HPLC with reasonable yields.

**Scheme 1.** Synthesis of the hit compound **2** and 4-arylthiazolyl piperidine analogs.<sup>a</sup>



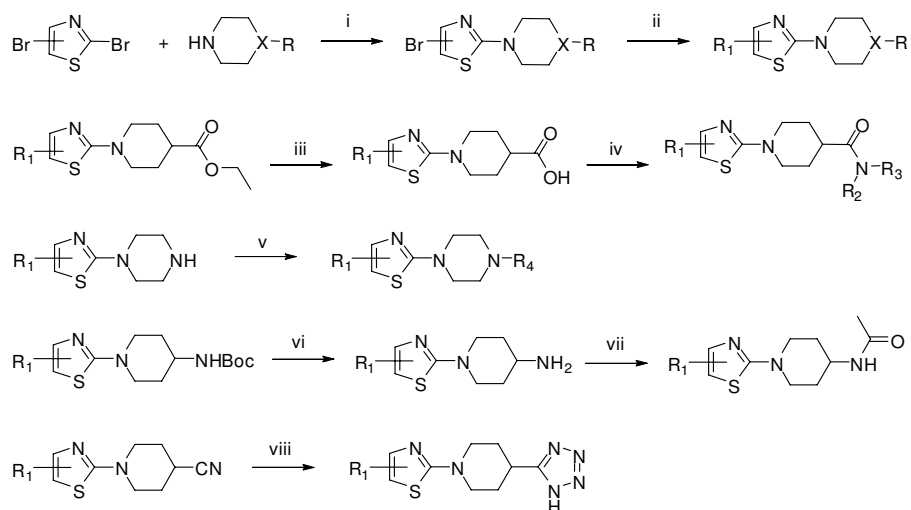
<sup>a</sup> Conditions and reagents: (i) triethylamine,  $\mu$ W, 100 or 120 °C; (ii) arylboronic acids or pinacol esters, 2.0 N Na<sub>2</sub>CO<sub>3</sub>, 5% Pd(PPh<sub>3</sub>)<sub>4</sub>,  $\mu$ W, 100 °C; (iii) a. 4-bromophenylboronic acid, 2.0 N Na<sub>2</sub>CO<sub>3</sub>, 5% Pd(PPh<sub>3</sub>)<sub>4</sub>,  $\mu$ W, 100 °C; b. MCPBA; (iv) triethylamine,  $\mu$ W, 100 or 120 °C.

**Scheme 2: Modifications at the thiazole core template.<sup>a</sup>**



<sup>a</sup> Conditions and reagents: (i) piperidine-4-carboxamide, triethylamine,  $\mu$ W, 100 or 120 °C; (ii) arylboronic acids or pinacol esters, 2.0 N  $\text{Na}_2\text{CO}_3$ , 5%  $\text{Pd}(\text{PPh}_3)_4$ ,  $\mu$ W, 100 °C; (iii) piperidine-4-carboxamide, *N,N*-diisopropylethylamine, 0 °C.

**Scheme 3: Synthesis of the piperidine modification analogs.<sup>a</sup>**



<sup>a</sup> Conditions and reagents: (i) dioxane, triethylamine,  $\mu$ W; (ii) arylboronic acids or pinacol esters, 2.0 N  $\text{Na}_2\text{CO}_3$ , 5%  $\text{Pd}(\text{PPh}_3)_4$ ,  $\mu$ W, 100 °C; (iii)  $\text{LiOH}$ , THF,  $\text{H}_2\text{O}$ ; (iv) EDC, DMAP,  $\mu$ W, 100 °C; (v)  $\text{KOCN}$ ,  $\text{H}_2\text{O}$ , or  $\text{R}_2\text{COCl}$ , triethylamine, or  $\text{R}_2\text{SO}_2\text{Cl}$ , triethylamine; (vi) trifluoroacetic acid, 54%; (vii) acetyl chloride, triethylamine; (viii)  $\text{ZnBr}_2$ ,  $\text{NaOH}$ , dioxane,  $\text{H}_2\text{O}$ , 120 °C.

### 2.3.2 Examples

General protocol A. A mixture of 1-(4-bromothiazol-2-yl)piperidine-4-carboxamide (0.100 mmol), boronic acid (0.200 mmol) and tetrakis(triphenylphosphine)palladium (5.00  $\mu$ mol) in DMF (1.50 mL) or CH<sub>3</sub>CN (1.50 mL) and 2.0 M Na<sub>2</sub>CO<sub>3</sub> aqueous solution (0.50 mL) was heated in  $\mu$ W at 100 °C for 30 min. The reaction was cooled to room temperature, and a small portion of Si-THIOL was added to get rid of palladium. The mixture was filtered through a frit to give light yellow solution. The crude material was submitted for HPLC purification under acidic or basic conditions to give the final product.

General protocol B. A mixture of carboxylic acid (0.082 mmol), EDC (0.082 mmol), HOBt (0.082 mmol), DMAP (0.082 mmol) and amine (0.163 mmol) in DMF (1.50 mL) was heated in  $\mu$ W at 100 °C for 1.5 h. The reaction mixture was subjected for HPLC purification under acidic or basic conditions to give the final product.

General protocol C. A solution of 4-(4-bromophenyl)-2-(piperazin-1-yl)thiazole (0.093 mmol), Et<sub>3</sub>N (0.139 mmol) in CH<sub>2</sub>Cl<sub>2</sub> (2.00 mL) was treated at 0 °C with carboxylic chloride or sulfonyl chloride (0.111 mmol). The reaction mixture was allowed to warm to room temperature, stirred for 1 h and concentrated. The crude mixture was subjected to HPLC separation under acidic or basic conditions to give the final product.

1-(4-(4-Bromophenyl)thiazol-2-yl)piperidine-4-carboxamide (CID 990823, 2). A general protocol for amination: A mixture of 2,4-dibromothiazole (2.06 g, 8.48 mmol), piperidine-4-carboxamide (1.30 g, 10.1 mmol) and TEA (2.50 mL) in ethanol (5.00 mL) was heated in  $\mu$ W at 100 °C for 1 hour. The reaction was cooled to room temperature, diluted with water and extracted with methanol and dichloromethane. The organic layer was separated, dried with Na<sub>2</sub>SO<sub>4</sub>, and concentrated as light brown solid. The crude mixture was purified by Biotage with 0-10% MeOH in CH<sub>2</sub>Cl<sub>2</sub> with 1% TEA to give 2.08 g (85%) of 1-(4-bromothiazol-2-yl)piperidine-4-carboxamide as a white solid: <sup>1</sup>H NMR (400 MHz, DMSO-*d*<sub>6</sub>)  $\delta$  ppm 7.31 (br. s., 1 H), 6.85 (s, 1 H), 6.82 (br. s., 1 H), 3.77 - 3.90 (m, 2 H), 3.03 (td, *J*=12.5, 2.8 Hz, 2 H), 2.29 - 2.39 (m, 1 H), 1.78 (dd, *J*=13.5, 3.1 Hz, 2 H), 1.50 - 1.63 (m, 2 H); LCMS RT = 4.134 min, *m/z* 289.9 [M+H<sup>+</sup>]. The title compound was prepared according to the general protocol A: <sup>1</sup>H NMR (400 MHz, DMSO-*d*<sub>6</sub>)  $\delta$  7.83-7.79 (m, 2 H), 7.59-7.55 (m, 2 H), 7.33 (s, 1 H), 7.32 (br. s., 1 H), 6.82 (br. s., 1 H), 3.96 (br. d., *J*=12.8 Hz, 2 H), 3.06 (td, *J*=12.6, 2.9 Hz, 2 H), 2.36 (tt, *J*=11.6, 3.8 Hz, 1 H), 1.82 (dd, *J*=13.0, 2.6 Hz, 2 H), 1.61 (qd, *J*=12.4, 4.0 Hz, 2 H); LCMS RT = 5.165 min, *m/z* 366.0 [M+H<sup>+</sup>]; HRMS (ESI) *m/z* calcd for C<sub>15</sub>H<sub>17</sub><sup>79</sup>BrN<sub>3</sub>OS [M+H<sup>+</sup>] 366.0276, found 366.0272.

1-(4-(4-Bromophenyl)thiazol-2-yl)-N-methylpiperidine-4-carboxamide (CID 46907665, 6a). The compound was prepared according to the general protocol B as a TFA salt: <sup>1</sup>H NMR (400 MHz, CHLOROFORM-*d*)  $\delta$  ppm 7.60 - 7.71 (m, 2 H), 7.47 - 7.57 (m, 2 H), 6.72 (s, 1 H), 5.78 (br. s., 1 H), 4.15 (dt, *J*=13.3, 3.5 Hz, 2 H), 3.10 - 3.30 (m, 2 H), 2.84 (d, *J*=5.1 Hz, 3 H), 2.41 (tt, *J*=11.1, 3.8 Hz, 1 H), 1.95 - 2.05 (m, 2 H), 1.81 - 1.95 (m, 2 H); <sup>19</sup>F NMR (376 MHz, CHLOROFORM-*d*)  $\delta$  ppm -75.97 (s); LCMS RT = 5.338 min, *m/z* 380.0 [M+H<sup>+</sup>]; HRMS (ESI) *m/z* calcd for C<sub>16</sub>H<sub>19</sub><sup>79</sup>BrN<sub>3</sub>OS [M+H<sup>+</sup>] 380.0432, found 380.0425.

1-(4-(4-Bromophenyl)thiazol-2-yl)piperidine-4-carboxylic acid (CID 3292095, **6k**). LiOH (1.01 g, 42.2 mmol) was added to a solution of ethyl 1-(4-(4-bromophenyl)thiazol-2-yl)piperidine-4-carboxylate (3.34 g, 8.45 mmol) in THF (24.0 mL) and H<sub>2</sub>O (8.00 mL) at room temperature. The reaction mixture was stirred at room temperature for 24 hours, diluted with 100 mL CH<sub>2</sub>Cl<sub>2</sub>, and washed with 2.0 N HCl (25.0 mL). The organic layer was separated, dried and concentrated to give a yellow oil. The crude product was purified by Biotage with 0-15% methanol in CH<sub>2</sub>Cl<sub>2</sub> to give 2.79 g (90%) product as a white solid. A small amount of sample was purified by HPLC under acidic condition to give the product as a TFA salt: <sup>1</sup>H NMR (400 MHz, DMSO-*d*<sub>6</sub>) δ ppm 7.74 - 7.88 (m, 2 H), 7.50 - 7.64 (m, 2 H), 7.33 (s, 1 H), 3.90 (dt, *J*=12.7, 3.5 Hz, 2 H), 3.04 - 3.23 (m, 2 H), 2.51 - 2.59 (m, 1 H), 1.94 (dd, *J*=13.1, 3.7 Hz, 2 H), 1.51 - 1.75 (m, 2 H); <sup>19</sup>F NMR (376 MHz, DMSO-*d*<sub>6</sub>) δ ppm -74.87 (s); LCMS RT = 5.841 min, *m/z* 367.0 [M+H<sup>+</sup>]; HRMS (ESI) *m/z* calcd for C<sub>15</sub>H<sub>16</sub><sup>79</sup>BrN<sub>2</sub>O<sub>2</sub>S [M+H<sup>+</sup>] 367.0116, found 367.0103.

2-(4-(1H-tetrazol-5-yl)piperidin-1-yl)-4-(4-bromophenyl)thiazole (CID 46907754, **6m**). A mixture of 1-(4-(4-bromophenyl)thiazol-2-yl)piperidine-4-carbonitrile (59.5 mg, 0.171 mmol), sodium azide (33.3 mg, 0.513 mmol) and zinc bromide (57.7 mg, 0.256 mmol) in water (1.00 mL) and 1,4-dioxane (0.58 mL). The pH of the solution was adjusted to about 7 with 1 N NaOH (~ 6 drops). The mixture was heated in an oil bath at 120 °C for 60 hours. Another aliquot of reagents was added and the mixture was re-heated at 120 °C for 60 hours. The mixture was cooled to room temperature, diluted with EtOAc and washed with H<sub>2</sub>O. The organic layer was separated, dried and concentrated in *vacuo*. The crude product was subjected to HPLC purification under basic conditions to give 15.0 mg (22%) product: <sup>1</sup>H NMR (400 MHz, DMSO-*d*<sub>6</sub>) δ ppm 7.76 - 7.87 (m, 2 H), 7.53 - 7.62 (m, 2 H), 7.33 (s, 1 H), 3.97 (dt, *J*=13.2, 3.7 Hz, 2 H), 3.20 - 3.30 (m, 2 H), 3.14 (tt, *J*=11.1, 3.6 Hz, 1 H), 2.04 (dd, *J*=13.3, 3.1 Hz, 2 H), 1.71 - 1.87 (m, 2 H); LCMS RT = 5.616 min, *m/z* 391.0 [M+H<sup>+</sup>]; HRMS (ESI) *m/z* calcd for C<sub>15</sub>H<sub>16</sub><sup>79</sup>BrN<sub>6</sub>S [M+H<sup>+</sup>] 391.0341, found 391.0338.

1-(4-(4-Bromophenyl)thiazol-2-yl)piperidin-4-amine (CID 46907724, **6n**). A solution of *tert*-butyl 1-(4-(4-bromophenyl)thiazol-2-yl)piperidin-4-ylcarbamate (78.7 mg, 0.180 mmol) in CH<sub>2</sub>Cl<sub>2</sub> (2.00 mL) was treated at 0 °C with TFA (1.00 mL). The mixture was stirred at 0 °C for 30 min and room temperature for 10 min. The solvents were removed under *vacuo*. The crude product was filtered through a short cartridge column to remove TFA salt to give 43.4 mg (72%) product as a white solid. A small portion of sample was re-purified by HPLC under acidic condition to give the product as a TFA salt: <sup>1</sup>H NMR (400 MHz, DMSO-*d*<sub>6</sub>) δ ppm 7.93 (br. s., 2 H), 7.72 - 7.85 (m, 2 H), 7.50 - 7.65 (m, 2 H), 7.37 (s, 1 H), 4.00 (d, 2 H), 3.25 - 3.35 (m, 1 H), 3.14 (td, *J*=12.8, 2.6 Hz, 2 H), 1.99 (dd, *J*=12.6, 3.0 Hz, 2 H), 1.57 (qd, *J*=12.4, 4.4 Hz, 2 H); <sup>19</sup>F NMR (376 MHz, DMSO-*d*<sub>6</sub>) δ ppm -73.54 (s); LCMS RT = 4.657 min, *m/z* 338.0 [M+H<sup>+</sup>]; HRMS (ESI) *m/z* calcd for C<sub>14</sub>H<sub>17</sub><sup>79</sup>BrN<sub>3</sub>S [M+H<sup>+</sup>] 338.0327, found 338.0323.

1-(4-(4-(4-Bromophenyl)thiazol-2-yl)piperazin-1-yl)ethanone (CID 46907737, **6t**). The compound was prepared according to the general protocol C as a TFA salt: <sup>1</sup>H NMR (400 MHz, CHLOROFORM-*d*) δ ppm 7.64 - 7.74 (m, 2 H), 7.47 - 7.55 (m, 2 H), 6.82 (s, 1 H), 3.77 - 3.92 (m, 2 H), 3.66 (br. s., 4 H), 3.48 - 3.58 (m, 2 H), 2.20 (s, 3 H); <sup>19</sup>F NMR (376 MHz, DMSO-*d*<sub>6</sub>) δ ppm -76.04 (s); LCMS RT = 5.892 min, *m/z* 366.0 [M+H<sup>+</sup>]; HRMS (ESI) *m/z* calcd for C<sub>15</sub>H<sub>17</sub><sup>79</sup>BrN<sub>3</sub>OS [M+H<sup>+</sup>] 366.0276, found 366.0274.

4-(4-(4-Bromophenyl)thiazol-2-yl)piperazine-1-carboxamide (CID 46907747, **6u**). A solution of 4-(4-bromophenyl)-2-(piperazin-1-yl)thiazole (40.0 mg, 0.123 mmol) in H<sub>2</sub>O (2.00 mL) was treated at room temperature with KOCN (20.0 mg, 0.247 mmol). The reaction mixture was stirred at room temperature

overnight. The mixture was extracted with EtOAc. The organic layer was separated, dried, and concentrated *in vacuo*. The crude mixture was subjected to HPLC separation under basic condition to give 14.2 mg product (31%) product:  $^1\text{H}$  NMR (400 MHz,  $\text{DMSO-}d_6$ )  $\delta$  ppm 7.82 (d,  $J=8.4$  Hz, 2 H), 7.57 (d,  $J=8.4$  Hz, 2 H), 7.37 (s, 1 H), 6.11 (br. s., 2 H), 3.37 - 3.57 (m, 8 H); LCMS RT = 5.329 min,  $m/z$  367.0  $[\text{M}+\text{H}^+]$ ; HRMS (ESI)  $m/z$  calcd for  $\text{C}_{14}\text{H}_{16}^{79}\text{BrN}_4\text{OS}$   $[\text{M}+\text{H}^+]$  367.0228, found 367.0215.

1-(4-(3-Isopropoxyphenyl)pyrimidin-2-yl)piperidine-4-carboxamide (CID 46907750, 7g). The compound was prepared according to the general protocol A as a TFA salt:  $^1\text{H}$  NMR (400 MHz,  $\text{DMSO-}d_6$ )  $\delta$  ppm 8.41 (d,  $J=5.1$  Hz, 1 H), 7.66 (ddd,  $J=8.1, 1.3, 1.0$  Hz, 1 H), 7.57 - 7.63 (m, 1 H), 7.41 (t,  $J=7.9$  Hz, 1 H), 7.29 (br. s., 1 H), 7.19 (d,  $J=5.3$  Hz, 1 H), 7.03 - 7.13 (m, 1 H), 6.78 (br. s., 1 H), 4.55 - 4.84 (m, 3 H), 2.88 - 3.10 (m, 2 H), 2.41 (tt,  $J=11.5, 3.8$  Hz, 1 H), 1.80 (dd,  $J=12.7, 2.9$  Hz, 2 H), 1.50 (qd,  $J=12.4, 3.9$  Hz, 2 H), 1.30 (d,  $J=6.1$  Hz, 6 H);  $^{19}\text{F}$  NMR (376 MHz,  $\text{DMSO-}d_6$ )  $\delta$  ppm -74.96 (s); LCMS RT = 4.454 min,  $m/z$  341.2  $[\text{M}+\text{H}^+]$ ; HRMS (ESI)  $m/z$  calcd for  $\text{C}_{19}\text{H}_{25}\text{N}_4\text{O}_2$   $[\text{M}+\text{H}^+]$  341.1978, found 341.1983.

1-(4-(3,4-Dihydro-2H-benzo[b][1,4]dioxepin-7-yl)pyrimidin-2-yl)piperidine-4-carboxamide (CID 46907738, 7h). The compound was prepared according to the general protocol A:  $^1\text{H}$  NMR (400 MHz,  $\text{DMSO-}d_6$ )  $\delta$  ppm 8.36 (d,  $J=5.1$  Hz, 1 H), 7.62 - 7.80 (m, 2 H), 7.29 (br. s., 1 H), 7.01 - 7.14 (m, 2 H), 6.78 (br. s., 1 H), 4.63 - 4.84 (m, 2 H), 4.10 - 4.26 (m, 4 H), 2.93 (td,  $J=12.7, 2.5$  Hz, 2 H), 2.40 (tt,  $J=11.5, 3.7$  Hz, 1 H), 2.14 (quin,  $J=5.6$  Hz, 2 H), 1.79 (dd,  $J=12.9, 2.7$  Hz, 2 H), 1.49 (qd,  $J=12.4, 4.3$  Hz, 2 H); LCMS RT = 3.836 min,  $m/z$  355.2  $[\text{M}+\text{H}^+]$ ; HRMS (ESI)  $m/z$  calcd for  $\text{C}_{19}\text{H}_{23}\text{N}_4\text{O}_3$   $[\text{M}+\text{H}^+]$  355.1770, found 355.1770.

1-(5-(3,4-Dihydro-2H-benzo[b][1,4]dioxepin-7-yl)thiazol-2-yl)piperidine-4-carboxamide (CID 46907699, 8a). The compound was prepared according to the general protocol A:  $^1\text{H}$  NMR (400 MHz,  $\text{DMSO-}d_6$ )  $\delta$  ppm 7.47 (s, 1 H), 7.31 (br. s., 1 H), 7.07 (d,  $J=2.3$  Hz, 1 H), 6.97 - 7.04 (m, 1 H), 6.89 - 6.96 (m, 1 H), 6.82 (br. s., 1 H), 4.12 (dt,  $J=9.3, 5.5$  Hz, 4 H), 3.89 (dt,  $J=12.8, 3.3$  Hz, 2 H), 3.04 (td,  $J=12.5, 2.9$  Hz, 2 H), 2.36 (tt,  $J=11.5, 3.7$  Hz, 1 H), 2.02 - 2.15 (m, 2 H), 1.79 (dd,  $J=13.2, 2.8$  Hz, 2 H), 1.50 - 1.68 (m, 2 H); LCMS RT = 3.735 min,  $m/z$  360.1  $[\text{M}+\text{H}^+]$ ; HRMS (ESI)  $m/z$  calcd for  $\text{C}_{18}\text{H}_{22}\text{N}_3\text{O}_3\text{S}$   $[\text{M}+\text{H}^+]$  360.1382, found 360.1379.

1-(5-(3,4-Dihydro-2H-benzo[b][1,4]dioxepin-7-yl)-1,3,4-thiadiazol-2-yl)piperidine-4-carboxamide (CID 46907746, 8b). The compound was prepared according to the general protocol A as a TFA salt:  $^1\text{H}$  NMR (400 MHz,  $\text{DMSO-}d_6$ )  $\delta$  ppm 7.23 - 7.52 (m, 3 H), 6.95 - 7.11 (m, 1 H), 6.84 (br. s., 1 H), 4.19 (t,  $J=5.6$  Hz, 4 H), 3.88 (dt,  $J=12.8, 3.5$  Hz, 2 H), 3.19 (td,  $J=12.4, 2.9$  Hz, 2 H), 2.35 (tt,  $J=11.4, 4.0$  Hz, 1 H), 2.14 (dt,  $J=11.2, 5.6$  Hz, 2 H), 1.82 (dd,  $J=13.5, 2.9$  Hz, 2 H), 1.65 (qd,  $J=12.4, 3.9$  Hz, 2 H);  $^{19}\text{F}$  NMR (376 MHz,  $\text{DMSO-}d_6$ )  $\delta$  ppm -74.79 (s); LCMS RT = 4.210 min,  $m/z$  361.1  $[\text{M}+\text{H}^+]$ ; HRMS (ESI)  $m/z$  calcd for  $\text{C}_{17}\text{H}_{21}\text{N}_4\text{O}_3\text{S}$   $[\text{M}+\text{H}^+]$  361.1334, found 361.1332.

1-(5-*p*-Polythiazol-2-yl)piperidine-4-carboxamide (CID 46907733, 8c). The compound was prepared according to the general protocol A as a TFA salt:  $^1\text{H}$  NMR (400 MHz,  $\text{DMSO-}d_6$ )  $\delta$  ppm 7.58 (s, 1 H), 7.34 - 7.45 (m, 2 H), 7.32 (br. s., 1 H), 7.18 (d,  $J=8.0$  Hz, 2 H), 6.84 (br. s., 1 H), 3.91 (dt,  $J=12.9, 3.2$  Hz, 2 H), 3.12 (td,  $J=12.6, 2.8$  Hz, 2 H), 2.38 (tt,  $J=11.4, 3.8$  Hz, 1 H), 2.29 (s, 3 H), 1.82 (dd,  $J=13.2, 2.8$  Hz, 2 H), 1.48 - 1.72 (m, 3 H);  $^{19}\text{F}$  NMR (376 MHz,  $\text{DMSO-}d_6$ )  $\delta$  ppm -74.86 (s); LCMS RT = 3.912 min,  $m/z$  302.1  $[\text{M}+\text{H}^+]$ ; HRMS (ESI)  $m/z$  calcd for  $\text{C}_{16}\text{H}_{20}\text{NOS}$   $[\text{M}+\text{H}^+]$  302.1327, found 302.1328.



1-(5-(3-Isopropoxyphenyl)thiazol-2-yl)piperidine-4-carboxamide (CID 46907708, **8l**). The compound was prepared according to the general protocol A as a TFA salt:  $^1\text{H}$  NMR (400 MHz, *DMSO-d*<sub>6</sub>)  $\delta$  ppm 7.65 (s, 1 H), 7.32 (br. s., 1 H), 7.24 (t, *J*=8.0 Hz, 1 H), 6.93 - 7.03 (m, 2 H), 6.83 (br. s., 1 H), 6.76 - 6.81 (m, 1 H), 4.55 - 4.75 (m, 1 H), 3.91 (dt, *J*=12.8, 3.4 Hz, 2 H), 3.11 (td, *J*=12.5, 2.9 Hz, 2 H), 2.37 (tt, *J*=11.4, 3.7 Hz, 1 H), 1.81 (dd, *J*=13.3, 2.9 Hz, 2 H), 1.52 - 1.68 (m, 2 H), 1.26 (d, *J*=6.1 Hz, 6 H);  $^{19}\text{F}$  NMR (376 MHz, *DMSO-d*<sub>6</sub>)  $\delta$  ppm -74.91 (s); LCMS RT = 4.300 min, *m/z* 346.1 [ $\text{M}+\text{H}^+$ ]; HRMS (ESI) *m/z* calcd for  $\text{C}_{18}\text{H}_{24}\text{N}_3\text{O}_2\text{S}$  [ $\text{M}+\text{H}^+$ ] 346.1589, found 346.1593.

1-(5-(4-(Methylthio)phenyl)thiazol-2-yl)piperidine-4-carboxamide (current updated 2<sup>nd</sup> probe, CID 46907676/ML200, **8m**). The compound was prepared according to the general protocol A as a TFA salt:  $^1\text{H}$  NMR (400 MHz, *DMSO-d*<sub>6</sub>)  $\delta$  ppm 7.58 (s, 1 H), 7.37 - 7.45 (m, 2 H), 7.32 (br. s., 1 H), 7.21 - 7.29 (m, 2 H), 6.83 (br. s., 1 H), 3.91 (dt, *J*=12.9, 3.0 Hz, 2 H), 3.09 (td, *J*=12.5, 2.8 Hz, 2 H), 2.48 (s, 3 H), 2.37 (tt, *J*=11.6, 4.0 Hz, 1 H), 1.81 (dd, *J*=13.5, 3.5 Hz, 2 H), 1.54 - 1.67 (m, 2 H);  $^{19}\text{F}$  NMR (376 MHz, *DMSO-d*<sub>6</sub>)  $\delta$  ppm -74.56 (s); LCMS RT = 4.072 min, *m/z* 361.1 [ $\text{M}+\text{H}^+$ ]; HRMS (ESI) *m/z* calcd for  $\text{C}_{16}\text{H}_{20}\text{N}_3\text{OS}_2$  [ $\text{M}+\text{H}^+$ ] 334.1048, found 334.1048.

1-(5-(3,4-Dihydro-2H-benzo[b][1,4]dioxepin-7-yl)thiazol-2-yl)piperidine-4-carboxylic acid (CID 46907666, **9a**). LiOH (86.0 mg, 3.60 mmol) was added to a solution of ethyl 1-(5-(3,4-dihydro-2H-benzo[b][1,4]dioxepin-7-yl)thiazol-2-yl)piperidine-4-carboxylate (284 mg, 0.72 mmol) in THF (6.00 mL) and H<sub>2</sub>O (2.00 mL) at room temperature. The reaction mixture was stirred at room temperature for 24 hours, diluted with 100 mL CH<sub>2</sub>Cl<sub>2</sub> and washed with 2 N HCl (25.0 mL). The organic layer was separated, dried and concentrated as a yellow oil. The crude was purified by Biotage with 0-15% methanol in CH<sub>2</sub>Cl<sub>2</sub> to give 233 mg (90%) product as a white solid:  $^1\text{H}$  NMR (400 MHz, *DMSO-d*<sub>6</sub>)  $\delta$  ppm 12.32 (br. s., 1 H), 7.48 (s, 1 H), 7.07 (d, *J*=2.2 Hz, 1 H), 6.97 - 7.03 (m, 1 H), 6.89 - 6.96 (m, 1 H), 4.12 (dt, *J*=9.2, 5.5 Hz, 4 H), 3.83 (ddd, *J*=13.2, 3.7, 3.5 Hz, 2 H), 2.98 - 3.20 (m, 2 H), 2.51 - 2.57 (m, 1 H), 2.04 - 2.17 (m, 2 H), 1.87 - 1.98 (m, 2 H), 1.49 - 1.69 (m, 2 H); LCMS RT = 4.177 min, *m/z* 361.1 [ $\text{M}+\text{H}^+$ ]; HRMS (ESI) *m/z* calcd for  $\text{C}_{18}\text{H}_{21}\text{N}_2\text{O}_4\text{S}$  [ $\text{M}+\text{H}^+$ ] 361.1222, found 361.1221.

1-(5-(3,4-Dihydro-2H-benzo[b][1,4]dioxepin-7-yl)thiazol-2-yl)-N-phenylpiperidine-4-carboxamide (CID 46907686, **9c**). The compound was prepared according to the general protocol A:  $^1\text{H}$  NMR (400 MHz, *DMSO-d*<sub>6</sub>)  $\delta$  ppm 9.95 (s, 1 H), 7.60 (dd, *J*=8.7, 1.1 Hz, 2 H), 7.49 (s, 1 H), 7.24 - 7.33 (m, 2 H), 6.97 - 7.11 (m, 3 H), 6.92 - 6.97 (m, 1 H), 4.13 (dt, *J*=9.4, 5.5 Hz, 4 H), 3.90 - 4.03 (m, 2 H), 3.10 (td, *J*=12.6, 2.7 Hz, 2 H), 2.62 (tt, *J*=11.5, 3.7 Hz, 1 H), 2.10 (quin, *J*=5.4 Hz, 2 H), 1.90 (dd, *J*=13.0, 2.8 Hz, 2 H), 1.71 (qd, *J*=12.4, 4.3 Hz, 2 H); LCMS RT = 4.936 min, *m/z* 436.2 [ $\text{M}+\text{H}^+$ ]; HRMS (ESI) *m/z* calcd for  $\text{C}_{24}\text{H}_{26}\text{N}_3\text{O}_3\text{S}$  [ $\text{M}+\text{H}^+$ ] 436.1695, found 436.1699.

### 3 Results

We designed a luciferase reporter gene assay by combining the promoter and splicing-based cassettes in tandem with the major portion of the native *SMN2* cDNA with luciferase. Earlier screening assays for SMA only targeted compounds that either stimulate the *SMN2* promoter or decrease exon 7 skipping. In this reporter, the *SMN2* promoter drives expression of luciferase reporter that is fused to an SMN splicing reporter (Figure 2). By including our SMN splicing cassette,<sup>xiii</sup> luciferase is only expressed when exon 7

is included in the mRNA transcript and the full-length protein is generated. This new assay can identify compounds that increase *SMN2* levels by three mechanisms: modulating alternative splicing of *SMN* exon 7, increasing transcription from the *SMN2* promoter, or, due to the presence of the native *SMN2* cDNA, stabilizing the *SMN* protein. The assay measures the luminescent signal produced by luciferase, and compounds that increase luminescent signaling will be flagged as potential actives.

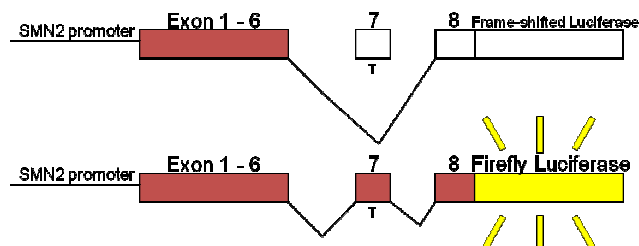


**Figure 2.** *SMN2*-luciferase reporter assay.

### 3.1 Summary of Screening Results

We performed this cell-based quantitative high-throughput screen (qHTS)<sup>xliii</sup> *SMN2*-luciferase reporter assay to identify compounds that increase expression of the full-length *SMN*-luciferase protein. The NIH Molecular Libraries of Small Molecule Repository<sup>xliiv</sup>, containing 210,386 compounds, was screened in the primary assay during the course of this screening campaign (Figure 3). We tested 1229 1536-well plates in the primary screen. The signal to background averaged 9 fold and the average *Z'* for the screen was 0.47 +/- 0.12, excluding 8 plates which failed visual QC. 6,128 compounds gave significant concentration-responses in the primary screen. Compounds were deprioritized for confirmation if they were suspected to interfere with the readout of the assay platform, or cellular viability using internal SAR data from other related assays. Recently, it has been brought to our attention that certain classes of luciferase inhibitors can stabilize the protein, and therefore appear as compounds able to increase the signal.<sup>xliv</sup> Compounds that act as luciferase inhibitors could show up in the *SMN2* assay as false positives due to this phenomenon. The vast majority of hits in the primary screen were luciferase inhibitors which presumably stabilized the *SMN2*-luciferase fusion protein and prevented cellular degradation – though this has not been explicitly proven. Select samples active in the primary screen were obtained in DMSO stock solutions from the MLSMR and/or as powders from compound vendors to confirm activity in the original assay. A homologous cell line harboring the *SMN1* gene fused to luciferase was used as a counter-screen. The *SMN1* reporter recapitulates the splicing pattern typically seen with the endogenous *SMN1* gene and predominately includes exon 7. Follow-up compounds that exhibit increased signal in the *SMN1* cell line were flagged as non-specific activators (i.e. transcription or protein stability). Purified luciferase enzyme was used in another counter-screen of the active compounds to filter off the potential false positives. A complete cheminformatics analysis of the follow up screening data included chemotype clustering, singleton identification, and structural considerations, including physical properties and optimization potential. In addition, potency range, maximum response, as well as the curve class<sup>xlvi</sup> was also considered. Ultimately, this analysis led us to select 21 candidates for further confirmation.

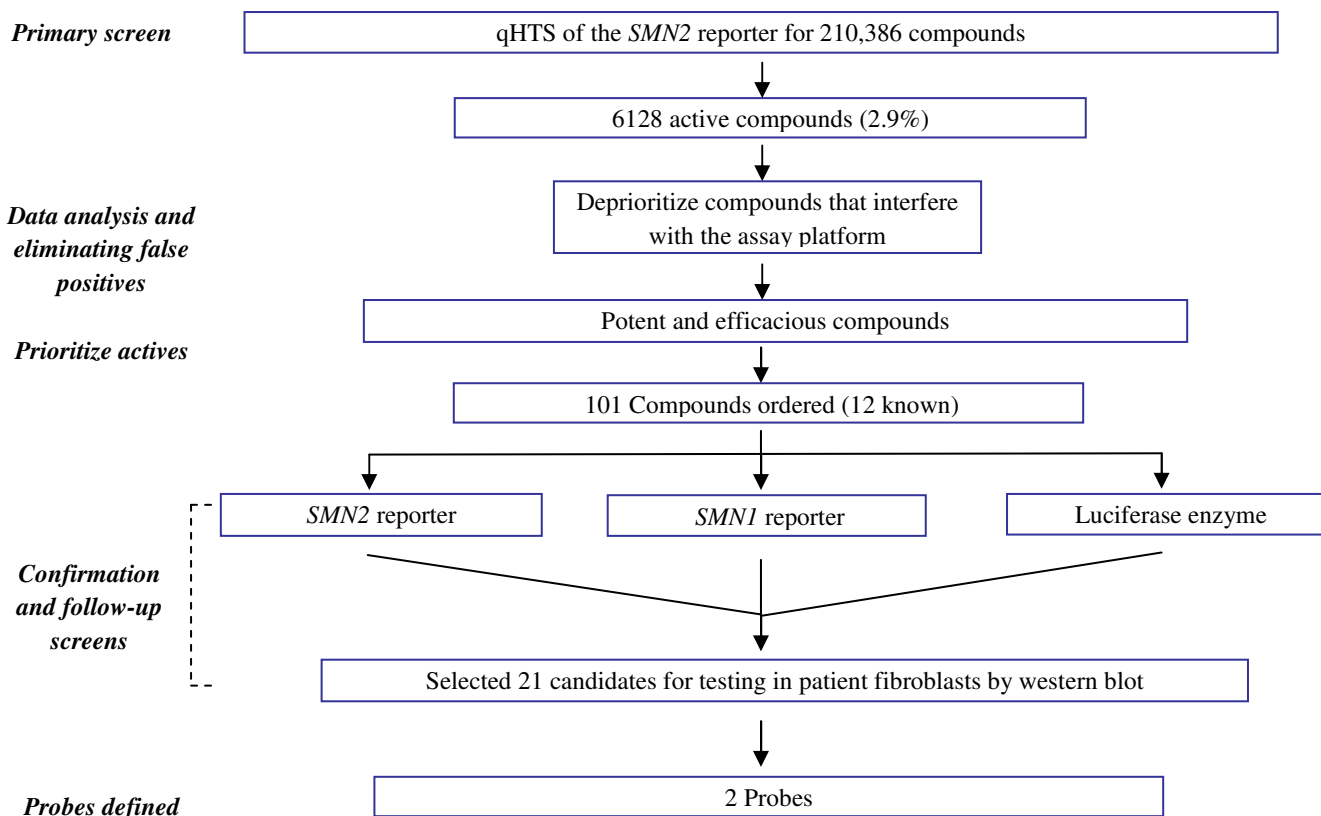


**Figure 3.** Overview of screening process.

Ideally, compounds modulating *SMN2* protein production in the luciferase reporter line would also modulate *SMN2* protein production in primary fibroblasts directly derived from SMA patients. Therefore, 21 compounds representing the diverse set of chemotypes confirmed from the primary screen were tested in a luciferase-free SMA-derived patient fibroblast assay for up-regulation *SMN* protein production by western blot. Ultimately, this campaign led us to focus on two lead series represented by the 5-methoxy-3,6-diphenyl-1,2,4-triazine (probe 1, CID 6404603, **1**) and 1-(4-(4-bromophenyl)thiazol-2-yl)piperidine-4-carboxamide (previous probe 2, CID 990823, **2**), which were able to increase the luciferase signal in the *SMN2* reported assay, and truly increase protein production in a dose-dependent manner in the western blot (Figure 4). In addition, although we do not know their specific mechanism of action, we noticed that the two active compounds **1** and **2** worked in a different mode, and distinct from compounds in the prior art. HDAC inhibitors and most compounds previously reported increased expression in both *SMN2* and *SMN1* reporter assays. Compound **1** increased the expression of *SMN2* and did not affect the expression of *SMN1*. On other hand, compound **2** increased the expression of *SMN2* but reduced the expression of *SMN1*. This reduction of *SMN1* expression would not be relevant *in vivo*, due to the fact that *SMN1* gene is not functional at all in SMA patients. The data in Figure 3 also showed the differences in luciferase inhibitory capacity of **1** and **2**. It can be seen that compound **1** is able to both increase the production of *SMN* protein (western) and inhibit luciferase, so without the creation of another cell line with a different reporter format, such as  $\beta$ -lactamase, GFP or Renilla luciferase, it would be impossible to discriminate between *SMN* upregulation and luciferase stabilization effects using our luciferase reporter assay. In

addition, the first triazine series chemotype was found to have a very narrow SAR. Therefore, we chose compound **2** as the prioritized series for further SAR optimization and biological evaluation since it possesses a more tractable SAR and drug-like properties. Furthermore, this series, as will later be shown, displayed highly permeability using Caco-2 cell assay,<sup>xlvii</sup> and it had with no indication of being a P-glycoprotein<sup>xlviii</sup> substrate.

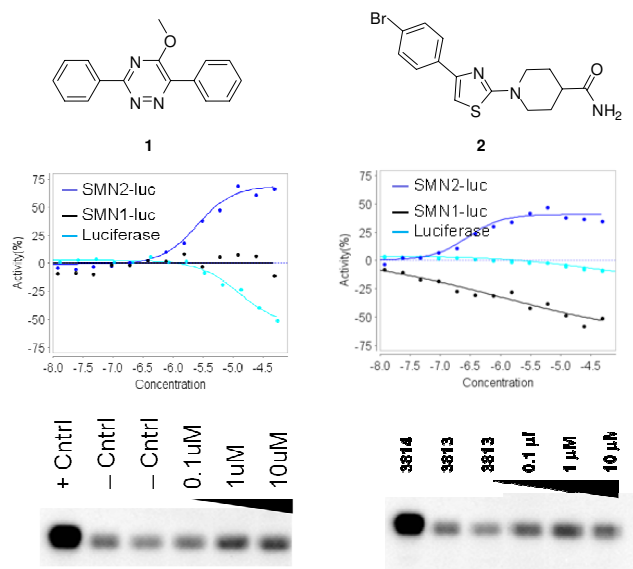


**Figure 4.** Hits from qHTS with follow up assays.

### 3.2 Dose Response Curves for Probe

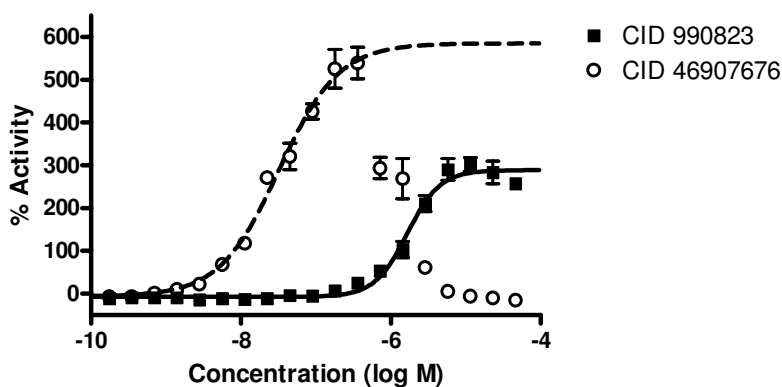


**Figure 5.** Dose response curves for current updated 2<sup>nd</sup> probe CID 46907676/ML200 (**8m**) and previous 2<sup>nd</sup> probe CID 990823 (**2**) in the SMN2-luciferase reporter assay.

Within our series, we observed a bell shape curve response, both in the primary reporter assay and other secondary assays such as western blot (please see Figure 6). This could be due with the intrinsic mechanism of action or to other causes, such as concentration dependent compound solubility.

### 3.3 Scaffold/Moiety Chemical Liabilities

This scaffold does not have any functional groups with potential chemical liabilities. Metabolic liabilities will be commented in the cellular activity part of the report (section 3.5).

### 3.4 SAR Tables

Tables 1-7 disclosed all the SAR data. The activity was reported showing two parameters: AC<sub>50</sub> (reflecting concentration necessary to reach 50% of maximum production) and rate of induction (referring to efficacy, maximum percentage of production with respect basal level), which were used to directly drive our SAR studies. It is important to evaluate and optimize both parameters because the ideal compound should maximize the SMN protein production at the minimum concentration.

As a standard practice, the hit compound **2** identified from the primary screen was re-synthesized and found to possess an AC<sub>50</sub> value of 1.22 μM with a rate of induction of 268%. Our early efforts were focused on improving both values and trying to further understand the SAR potential and limitation of this chemotype. In order to explore the space and the electronic effects of aromatic substituents, we held the thiazole and piperidine ring constant and did a comprehensive SAR investigation of the aromatic substituents at the 4-position of the thiazole core ring as shown in Table 1. We first examined the effect of the substituent position of the phenyl ring on the potency and efficacy. In general, most of *ortho*-substituents at the phenyl ring yielded analogs which were less active both in AC<sub>50</sub> and rate of induction (analogs **3b**, **3e**, **3o**, **3u**, **4a**, **4c**, **4g**, **4m**, **4p**), with the exception of the *ortho*-fluoro substitution analog **3r** (AC<sub>50</sub> = 2.44 μM, rate of induction = 274%). This data indicated the potential necessity of having a coplanar conformation between the two aromatic rings for maintaining good activity. In contrast to *ortho*-substitutions, substituents at *meta* or *para* positions were generally tolerated. As for the electronic nature of the substituents, we found that electron-donating functional groups at the *meta* or *para* position tended to provide better activity and efficacy than the corresponding electron-withdrawing groups. In addition, halo, methyl or trifluoromethyl substitutions at the *para* and *meta* position were also tolerated. Several aromatic substitutions slightly increased or almost maintained the activity and the efficacy of the hit compound **2**, such as *meta*-methoxy substituted analog **3c** (AC<sub>50</sub> = 1.94 μM, rate of induction = 357%), *meta*-*N,N*-dimethylamino substituted analog **3f** (AC<sub>50</sub> = 0.97 μM, rate of induction = 504%), and *para*-methyl substituted analog **3m** (AC<sub>50</sub> = 1.22 μM, rate of induction = 439%). Regarding hetero-aromatic ring substituents, none of the analogs (**4s-4u**) had a positive impact on either the activity or efficacy of the parent molecule. We also studied several polycyclic aromatic rings analogs (**4e**, **4f**, **4v-4x**). However, most of them had either no activity or decreased activity and efficacy.

From here, given the improved potency and efficacy observed with the electron-donating substituents, we chose to screen the large number of phenoxy substituents (Table 2). Several electron-donating substituents were tolerated including *meta*-isopropylphenyl (analog **5c**, AC<sub>50</sub> = 0.77 μM, rate of induction = 605%). We also examined the 3,5- or 3,4-disubstituted analogs (**5h** and **5i**, AC<sub>50</sub> = 7.72 μM and 12.24 μM, rate of induction = 45% and 59%, respectively) and 3,4,5-trisubstituted derivative (analog **5m**, AC<sub>50</sub> = 19.4 μM, rate of induction = 73%). Surprisingly, these modifications resulted in a huge loss of both activity and efficacy. Interestingly, this severe loss could be regained by bridging two substituents together. Furthermore, the resulting cyclic poly-phenolic-ethers showing a clear trend of improvement in

activity in line with ring size ( $5 < 6 < 7$ , analogs **5j**, **5k**, **5l**,  $AC_{50} = 2.44 \mu\text{M}$ ,  $0.77 \mu\text{M}$ , and  $0.49 \mu\text{M}$ , respectively).

With several improved analogs derived from the aromatic modification in hand (analog **5c**, **5k**, **5l**), we further studied the SAR of the piperidine ring moiety as shown in Table 3. In general, mono or disubstituted amide derivatives (represented analogs **6a-6i**) were found to have worse potency and efficacy numbers, with the exception of the phenylamide derivative (analog **6e**,  $AC_{50} = 2.44 \mu\text{M}$ , rate of induction = 262%) that is about the same as the hit compound **2**. It was also important that both the carboxylic acid as well as the corresponding ethyl ester derivative retained acceptable levels of potency and improved efficacy (analog **6k** and **6j**,  $AC_{50} = 4.87 \mu\text{M}$  and  $7.72 \mu\text{M}$ , rate of induction = 554% and 550%, respectively). This result pointed to the direction that probably only the carbonyl functional group might be involved in a potential hydrogen bond interaction. This was further confirmed by significant loss of potency of the amide trunked analogs **6q-6s**. When the amide moiety was replaced by cyano or tetrazole groups, the resulting derivatives (analog **6l** and **6m**) also showed a loss of potency. A reversed amide (analog **6o**) or carbamate (analog **6p**) could not be tolerated, while a free amine moiety seemed to be tolerated (analog **6n**,  $AC_{50} = 2.44 \mu\text{M}$ , rate of induction = 182%). In contrast to the modification of the amide moiety, the piperidine ring was found to be necessary to maintain potency, with an exemption of analog **6t**, which had another version of the reversed amide of the original hit compound **2**. Derivatives from piperazine replacement were examined and resulted in mostly inactive analogs (**6u-6y**).

In general, replacing the thiazole ring by a pyrimidine maintained the potency and efficacy (Table 4). Having the piperidine-4-carboxamide substituent between the two hetero-aromatic nitrogen atoms and aromatic substituent at 4-position, increased the potency of the molecule by 2-3 fold (analog **7d**,  $AC_{50} = 0.387 \mu\text{M}$ , rate of induction = 387%; analog **7i**,  $AC_{50} = 0.772 \mu\text{M}$ , rate of induction = 446%). The aromatic substituent at 5 position of the pyrimidine was also tolerated as represented by analog **7b**, although the efficacy was only half in comparison with the above described pyrimidine analogs ( $AC_{50} = 0.613 \mu\text{M}$ , rate of induction = 236%). The *meta*-isopropylphenyl substitution derivative (analog **7g**) was found to be the best in the series with an  $AC_{50} = 0.154 \mu\text{M}$ , which was close to a 9 fold increase in potency. A derivative from monofluoro substituent at 5 position of the pyrimidine improved potency by additional 2-4 fold (analog **7j** vs analog **7i**; analog **7l** vs analog **7n**). While additional nitrogen around the pyrimidine ring (1,3,5-triazine replacement) resulted in a decrease of potency (analog **7i** vs analog **7k**; analog **7h** vs analog **7p**). These results indicated that the potency of the parent compounds would benefit from the electron deficiency of the pyrimidine core ring. An *ortho* methyl substituted derivative (analog **7o**) was found to be totally inactive which was echoed with the previous finding about the co-planar conformation. On the other hand, when the pyrimidine substitution patterns were reversed, with the aromatic substituent between the two hetero-aromatic nitrogen atoms and the piperidine-4-carboxamide substituent at position 4, the resulting derivatives decreased activity by 8-16 fold (analog **7i** vs analog **7n**; analog **7j** vs analog **7l**). In addition, moving two nitrogen atoms around the pyrimidine also ended the decreasing the potency by 5 fold (analog **7i** vs analog **7m**; analog **7h** vs analog **7q**). This finding reinforced our prediction that hydrogen bond interactions were produced when a sterically accessible nitrogen as hydrogen bond acceptor was placed next to the piperidine functional group.

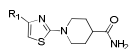
Table 5 showed further modifications we performed for studying the SAR for the thiazole core. Switching the aromatic substituent from the 4 position to 5 position of the thiazole core ring dramatically boosted 5

fold of magnitude the potency and almost doubled the efficacy (analog **8g**,  $AC_{50}$  = 0.224  $\mu$ M, rate of induction = 599%). Again, we speculated that this increment was due to the creation of a new hydrogen bond interaction with the thiazole nitrogen. Addition of one more nitrogen atom to the thiazole ring (1,3,4-thiadiazole replacement) resulted in a 3-10 fold loss of potency (analog **8a** vs analog **8b**; analog **8c** vs analog **8d**; analog **8e** vs analog **8f**; analog **8g** vs analog **8h**). This result agreed with the SAR findings in the pyrimidine system due to the electronic effect of the core ring.

With a hope that the previous SAR of the aromatic substituents could be translated from 2,4-substituted thiazole to 2,5-substituted system, a fine tune SAR of the different electron-donating groups on the phenyl moiety was explored (Table 5 and Table 6). Gratifyingly, several electron-donating groups on the phenyl ring indeed have the synergic effect on both potency and efficacy (represented by analog **8a**,  $AC_{50}$  = 0.039  $\mu$ M, rate of induction = 370%; analog **8e**,  $AC_{50}$  = 0.039  $\mu$ M, rate of induction = 550%; analog **8l**,  $AC_{50}$  = 0.077  $\mu$ M, rate of induction = 709%; and analog **8m**,  $AC_{50}$  = 0.031  $\mu$ M, rate of induction = 576%). The 3,4-disubstituted derivative **8n** again was less active than the corresponding ring closed analogs **8o-8q**. Several cyclic *meta-N,N*-disubstituted aminophenyl derivatives (analog **8r-8t**) were examined and were found to be less active than the parent *meta-N,N*-dimethylaminophenyl derivative (analog **8e**).

The modification of the amide moiety in the 2,5-substituted thiazole system was further explored, as shown in Table 7. For these studies, we retained 3,4-dihydro-2H-benzo[b][1,4]dioxepin-7-yl and *meta-N,N*-dimethylaminophenyl as two aromatic substituents and thiazole core ring to provide comparative uniformity. The results demonstrated that the replacement of amide with acid had clear advantage on potency with a 3-fold improvement, but with a slight loss of efficacy (analog **9a** with best  $AC_{50}$  = 0.012  $\mu$ M, rate of induction = 325%). Ethyl ester or phenylamide derivatives were also tolerated (analog **9b**,  $AC_{50}$  = 0.031  $\mu$ M, rate of induction = 320%; analog **9c**,  $AC_{50}$  = 0.049  $\mu$ M, rate of induction = 353%). However, the imidazole and methylketone replacements were not tolerated (analog **9d**, **9e**, **9g**, and **9h**). Using a luciferase reporter assay to drive our medicinal chemistry efforts, we created a large pool of potent analogs after several round of SAR studies.

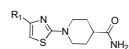
**Table 1:** SAR of 2,4-substituted thiazole aromatic analogs containing an aromatic substituent.



#	CID	SID	NOGC	R <sub>1</sub>	AC <sub>50</sub> (μM)	Rate of induction (%)
2	990823	87677807	NOGC00183633-01		1.22	268
3a	4084587	99867889	NOGC00183652-01		7.72	167
3b	49907682	99867900	NOGC00183653-01		inactive	inactive
3c	49907716	99867908	NOGC00183672-01		1.84	357
3d	44144332	87677815	NOGC00183648-01		7.72	209
3e	44144362	87677821	NOGC00183659-01		inactive	inactive
3f	44144366	87677824	NOGC00183664-01		0.97	504
3g	49907722	99867943	NOGC00184845-01		30.74	64
3h	49907751	99867902	NOGC00183660-01		6.13	100
3i	44144360	87677820	NOGC00183657-01		inactive	inactive
3j	49907727	99867927	NOGC00184825-01		inactive	inactive
3k	49907660	99867903	NOGC00183661-01		inactive	inactive
3l	49907701	99867910	NOGC00183676-01		30.74	187
3m	44143947	87677833	NOGC00183662-01		1.22	439
3n	49907683	99867941	NOGC00184843-01		3.87	243
3o	44144340	87677812	NOGC00183643-01		inactive	inactive
3p	49907696	99867926	NOGC00184824-01		387	100
3q	49907749	99867889	NOGC00183627-01		2.44	386
3r	44144338	87677811	NOGC00183640-01		2.44	274
3s	49907693	99867892	NOGC00183639-01		9.72	64
3t	44143946	87677806	NOGC00183631-01		3.87	288
3u	49907717	99867894	NOGC00183642-01		7.72	57
3v	44144336	87677827	NOGC00183671-01		12.24	53
3w	802475	99867893	NOGC00183641-01		2.44	381

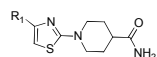


**Table 1 continued:** SAR of 2,4-substituted thiazole aromatic analogs containing an aromatic substituent.



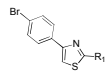
#	CID	SID	NGGC	R <sub>1</sub>	AC <sub>50</sub> (μM)	Rate of induction (%)
4a	44144334	87677816	NGGC00183549-01		inactive	inactive
4b	46907691	99367896	NGGC00183547-01		30.75	57
4c	44143159	87677823	NGGC00183563-01		inactive	inactive
4d	46907711	99367897	NGGC00183550-01		24.42	58
4e	630762	99367912	NGGC00183576-01		inactive	inactive
4f	44143948	87677810	NGGC00183537-01		7.72	162
4g	44144342	87677813	NGGC00183544-01		inactive	inactive
4h	44143157	87677828	NGGC00183573-01		inactive	inactive
4i	46907760	99367907	NGGC00183570-01		inactive	inactive
4j	44144358	87677819	NGGC00183556-01		3.87	356
4k	44144344	87677829	NGGC00183575-01		12.24	130
4l	44144364	87677825	NGGC00183565-01		12.24	51
4m	46907706	99367895	NGGC00183545-01		inactive	inactive
4n	46907719	99367909	NGGC00183574-01		3.87	20
4o	800332	99367898	NGGC00183551-01		15.41	254
4p	46907684	99367904	NGGC00183566-01		inactive	inactive
4q	46907742	99367901	NGGC00183558-01		inactive	inactive
4r	46907731	99367906	NGGC00183569-01		9.72	49
4s	44144350	87677832	NGGC00183581-01		7.72	51
4t	44144352	87677817	NGGC00183554-01		inactive	inactive
4u	44144356	87677814	NGGC00183546-01		inactive	inactive
4v	44144368	87677822	NGGC00183562-01		7.72	534
4w	44144370	87677826	NGGC00183567-01		15.41	100
4x	46907675	99367891	NGGC00183538-01		30.74	369

**Table 2.** SAR of 2,4-substituted thiazole aromatic analogs containing a phenoxy substituent.



#	CID	SID	NCGC	R <sub>1</sub>	AC <sub>50</sub> (μM)	Rate of induction (%)
2	990823	87677807	NCGC00183533-01		1.22	268
3a	4084597	99367899	NCGC00183552-01		7.72	167
3b	46907682	99367900	NCGC00183553-01		inactive	inactive
3c	46907716	99367908	NCGC00183572-01		1.94	357
3d	44144332	87677815	NCGC00183548-01		7.72	209
5a	46907744	99367939	NCGC00184940-01		3.07	297
5b	46907757	99367940	NCGC00184941-01		3.87	212
5c	46907658	99367948	NCGC00184953-01		0.77	605
5d	46907689	99367935	NCGC00184936-01		3.87	178
5e	46907705	99367947	NCGC00184952-01		3.07	54
5f	46907681	99367936	NCGC00184937-01		4.87	240
5g	46907743	99367938	NCGC00184939-01		inactive	inactive
5h	46907659	99367930	NCGC00184928-01		7.72	45
5i	46907680	99367928	NCGC00184926-01		12.24	59
5j	46907672	99367911	NCGC00183577-01		2.44	359
5k	44144346	87677830	NCGC00183579-01		0.77	459
5l	46907714	99367942	NCGC00184944-01		0.49	443
5m	46907669	99367929	NCGC00184927-01		19.40	73
5n	46907734	99367937	NCGC00184938-01		12.24	401
5o	44144348	87677831	NCGC00183580-01		15.41	589

**Table 3.** SAR of 2,4-substituted thiazole analogs containing modifications of the primary amide moiety and piperidine ring.



#	CID	SID	NCGC	R <sub>1</sub>	AC <sub>50</sub> (μM)	Rate of induction (%)	#	CID	SID	NCGC	R <sub>1</sub>	AC <sub>50</sub> (μM)	Rate of induction (%)
2	990823	87677807	NCGC00183533-01		1.22	268	6m	46907754	99367952	NCGC00184958-01		12.24	67
6a	46907665	99367913	NCGC00184909-01		7.72	101	6n	46907724	99367951	NCGC00184957-01		2.44	182
6b	46907723	99367914	NCGC00184910-01		30.75	43	6o	46907674	99367953	NCGC00184959-01		15.41	-57
6c	46907697	99367917	NCGC00184911-01		30.75	77	6p	46907667	99367945	NCGC00184948-01		inactive	inactive
6d	46907661	99367918	NCGC00184915-01		inactive	inactive	6q	2900985	87677809	NCGC00183536-01		19.40	272
6e	46907736	99367915	NCGC00184911-01		2.44	262	6r	720656	87677808	NCGC00183534-01		inactive	inactive
6f	46907707	99367916	NCGC00184912-01		inactive	inactive	6s	46907740	99367949	NCGC00184954-01		24.42	-97
6g	46907721	99367919	NCGC00184916-01		6.13	32	6t	46907737	99367950	NCGC00184956-01		3.07	234
6h	46907690	99367920	NCGC00184917-01		inactive	inactive	6u	46907747	99367958	NCGC00184964-01		12.24	89
6i	46907726	99367921	NCGC00184918-01		inactive	inactive	6v	46907688	99367954	NCGC00184960-01		inactive	inactive
6j	46907735	99367890	NCGC00183535-01		7.72	550	6w	46907709	99367955	NCGC00184961-01		inactive	inactive
6k	3292095	99367905	NCGC00183568-01		4.87	554	6x	46907673	99367956	NCGC00184962-01		inactive	inactive
6l	46907752	99367944	NCGC00184947-01		30.74	78	6y	46907730	99367957	NCGC00184963-01		inactive	inactive

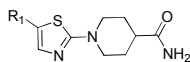
**Table 4.** SAR of analogs containing modifications of thiazole core.

#	CID	SID	NCGC	Structure	AC <sub>50</sub> (μM)	Rate of induction (%)
7a	46907712	99367923	NCGC00184920-01		inactive	inactive
7b	46907753	99367933	NCGC00184932-01		0.613	236
7c	46907729	99367924	NCGC00184921-01		inactive	inactive
7d	46907715	99367925	NCGC00184923-01		0.387	387
7e	46907685	99367989	NCGC00187895-01		0.387	444
7f	46907663	99367964	NCGC00187854-01		1.22	364
7g	46907750	99367990	NCGC00187896-01		0.154	298
7h	46907738	99367963	NCGC00187853-01		1.54	234
7i	46907720	99367934	NCGC00184933-01		0.772	446
7j	46907704	99367981	NCGC00187873-01		0.387	373
7k	46907725	99367977	NCGC00187869-01		1.22	200
7l	46907756	99367984	NCGC00187876-01		3.07	141
7m	46907758	99367975	NCGC00187867-01		3.87	81
7n	46907656	99367946	NCGC00184949-01		12.24	306
7o	46907700	99367979	NCGC00187871-01		inactive	inactive
7p	46907710	99367976	NCGC00187868-01		2.44	186
7q	46907671	99367974	NCGC00187866-01		7.72	211

**Table 5.** SAR of analogs having 2,5-substituted thiazole and thiadiazole cores.

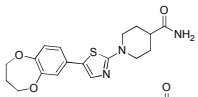
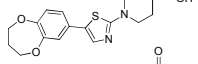
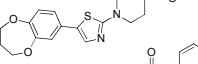
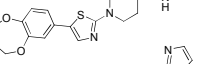
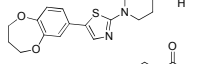
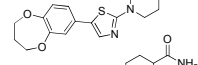
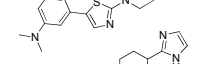
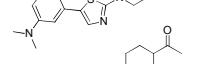
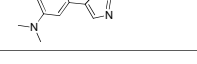
#	CID	SID	NCGC	Structure	AC <sub>50</sub> (μM)	Rate of induction (%)
8a	46907699	99367961	NCGC00187851-01		0.038	370
8b	46907746	99367991	NCGC00187897-01		0.122	257
8c	46907733	99367986	NCGC00187892-01		0.077	609
8d	46907692	99367967	NCGC00187857-01		0.244	54
8e	46907664	99367932	NCGC00184931-01		0.038	550
8f	46907677	99367966	NCGC00187856-01		0.387	448
8g	46907662	99367931	NCGC00184930-01		0.244	599
8h	46907670	99367965	NCGC00187855-01		inactive	inactive

**Table 6.** SAR of 2,5-substituted thiazole aromatic analogs containing an aromatic substituent.



#	CID	SID	NCGC	R <sub>1</sub>	AC <sub>50</sub> (μM)	Rate of induction (%)
8i	46907713	99367922	NCGC00184919-01		inactive	inactive
8g	46907662	99367931	NCGC00184930-01		0.244	599
8j	46907728	99367987	NCGC00187893-01		0.154	498
8k	46907745	99367960	NCGC00187850-01		2.44	601
8c	46907733	99367986	NCGC00187892-01		0.077	609
8l	46907708	99367988	NCGC00187894-01		0.077	709
8e	46907664	99367932	NCGC00184931-01		0.039	550
8m	46907676	99367992	NCGC00187898-01		0.031	576
8n	46907678	99367982	NCGC00187874-01		9.72	209
8o	46907748	99367962	NCGC00187852-01		0.049	590
8p	46907698	99367959	NCGC00187849-01		0.097	424
8a	46907699	99367961	NCGC00187851-01		0.039	370
8q	46907695	99367994	NCGC00187900-01		0.194	598
8r	46907702	99367969	NCGC00187859-01		0.387	685
8s	46907679	99367970	NCGC00187860-01		1.54	565
8t	46907657	99367971	NCGC00187861-01		2.44	275

**Table 7.** SAR of 2,5-substituted thiazole analogs containing modifications at the primary amide.

#	CID	SID	NCGC	Structure	AC <sub>50</sub> (μM)	Rate of induction (%)
8a	46907699	99367961	NCGC00187851-01		0.039	370
9a	46907666	99367980	NCGC00187872-01		0.012	325
9b	46907687	99367978	NCGC00187870-01		0.031	320
9c	46907686	99367983	NCGC00187875-01		0.049	353
9d	46907732	99367968	NCGC00187858-01		2.44	129
9e	46907741	99367972	NCGC00187864-01		inactive	inactive
8e	46907664	99367932	NCGC00184931-01		0.039	550
9f	46907703	99367993	NCGC00187899-01		7.72	188
9g	46907755	99367973	NCGC00187865-01		3.07	224

## Secondary Validation Assays

With the SAR assessment established for this series, a number of selected analogs featuring desirable *SMN2* potency below 150 nM in the reporter assay were then examined to evaluate the effect on the human SMN protein expression using fibroblasts from SMA patients. We incubated a fibroblast cell line from a type I SMA patient (3813 cell line) with different doses of analogs and assessed the SMN protein level by quantitative western blotting (Figure 6). We observed that the probe compound **8m** at concentration of 37 nanomolar increased the SMN protein level by 2-3 fold. The SMN protein level was decreased with the increasing of the drug concentration. This result matched with of bell-shaped curve observed in the luciferase reporter assay. Analog **9a** showed a dose-dependent trend between 37 nM to 1 μM concentration and a decrease of protein level at 3 μM. Other selected agents (**9c**, **8c** and **8l**) all showed an up-regulation of SMN protein at concentrations ranging between 37 nM and 333 nM.

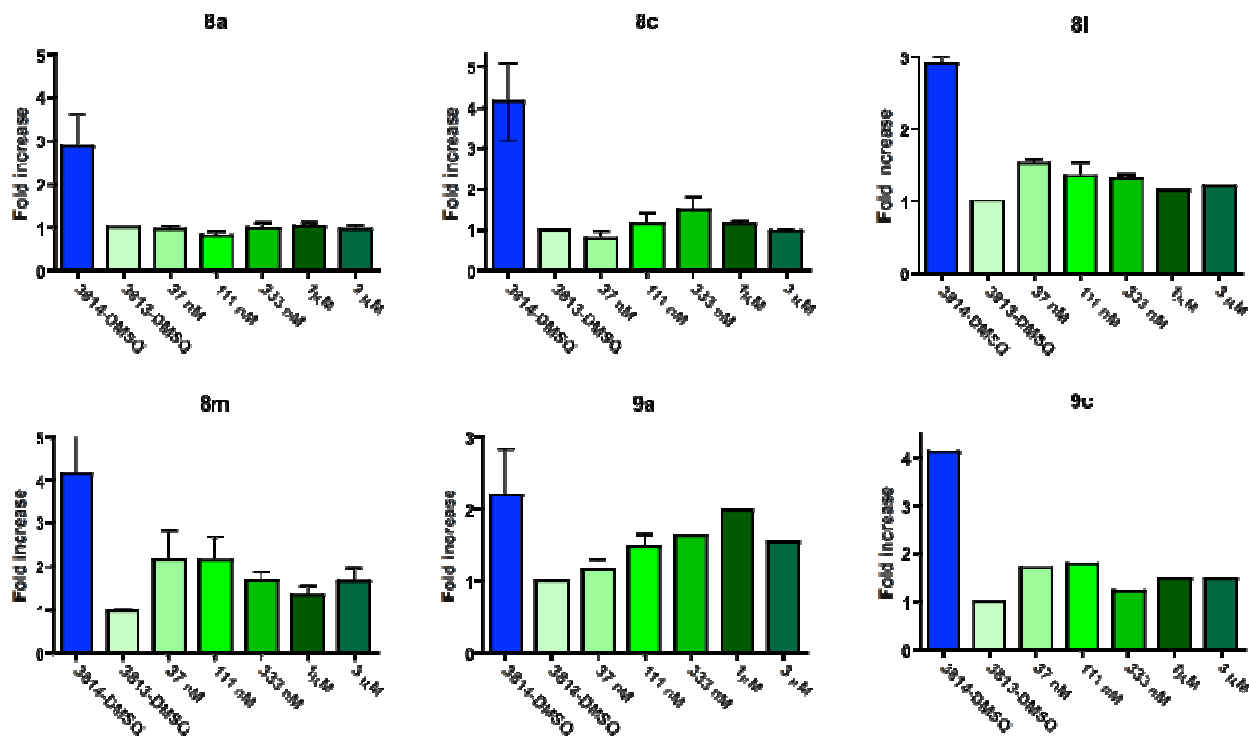


**Figure 6.** Quantification of western blot of SMN levels after treatment with drug compounds as indicated with different doses.

Furthermore, the increase in SMN protein production led us to explore whether the arylpiperidine analogs had effect of on the overall number of SMN positive foci or gems in the nucleus. This would corroborate that the increased protein amounts represent indeed functional SMN protein. SMN protein is predominately a cytoplasmic protein in the nucleus SMN that localized in distinct punctuate bodies often referred to as gems (gemini of coiled [Cajal] bodies). There is a direct correlation between the number of gems and total SMN protein production in the cell. Gem counts are commonly used as another metric to score the amount total SMN protein expressed on a cell to cell basis. The number of nuclei with gems and the number of gems per cell were both significantly reduced in type I SMA cells.<sup>xlix</sup> Only 3.3% of nuclei have gems in fibroblast cells from SMA type I patients (cell line 3813), while 24.8% of nuclei have gems in fibroblast from a carrier parent (3814 cell line). We treated human type I SMA fibroblasts with increasing doses (37 nM – 3000 nM) of arylpiperidine analogs **8a**, **8m**, and **9a** for 3 days and the number of gems per 100 nuclei were examined (Figure 7). The probe compound **8m** treatment yielded more than 2 fold of increase of the number of the gems at low 37 nM doses. With the concentration increased, the numbers of gems was reduced which agreed with the previous findings. Analog **9a** also showed an 80% increase of the gem numbers at 37 nM to 1000 nM concentrations and slightly decreased at 3000 nM. However, analog **8a** didn't show any activity in this assay.



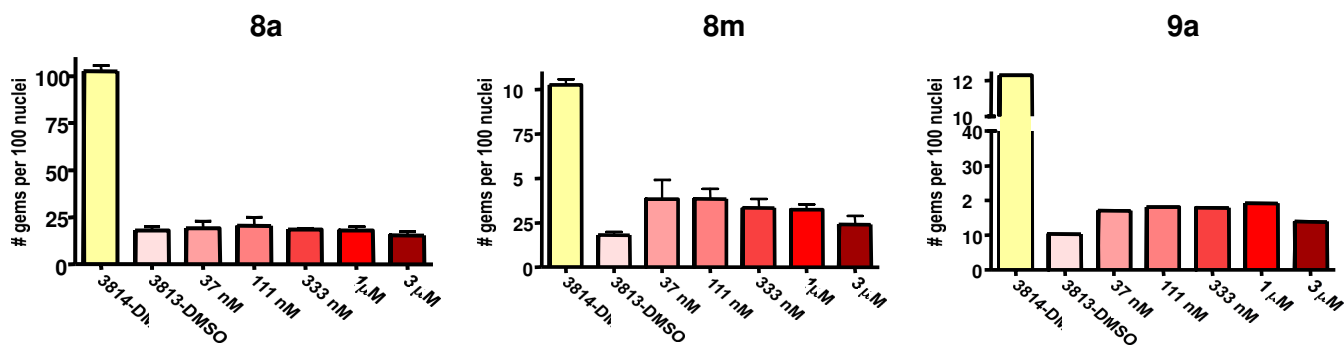


**Figure 7.** Number of gems per 100 nuclei after treatment with drug compounds as indicated with different doses.

### 3.5 Cellular Activity

In the previous section (Secondary Validation Assays), we already presented the activity of some of our best compounds, including the current 2<sup>nd</sup> probe compound **8m** in cell base assays with patient fibroblasts, increasing the production of SNM protein and the number of gems bodies. Currently, we are in the process of evaluating our compounds directly in motor neurons derivate from SMA iPSC, and testing their capacity of impacting SNM production, gems count and survival. We will update the probe report with those data as soon we obtain them.

In addition, several of the most potent analogs were profiled of mouse liver microsomal stability and permeability in Caco-2 cells (Table 8). For the microsomal stability, we decided to evaluate the remaining amount of our compounds upon incubation at thee different time periods: 10, 15 and 60 minutes. This allowed us to calculate both the intrinsic clearance and their half lives. The original 2<sup>nd</sup> probe compound **2** was found to have a relative short half life time of 12 minutes. Analogs **8c**, and **9c** all had a very short half life time of less than 10 minutes, as well as the current 2<sup>nd</sup> probe compound **8m**. Analogs **8b**, **8l** and **9a** owned a half life time of more than 30 minutes. In the Caco-2 permeability assay, analogs **7g**, **8b**, and **9a** were found to be very high permeable, while analog **8l** had a very promising efflux ratio of 0.049. However, the permeability of the current 2<sup>nd</sup> probe compound **8m** was not great, though the efflux ratio was decent (0.125). In consideration of a balance of potency, efficacy, ADMET properties of all current analogs, we selected another analog **8l** for *in vivo* pharmacokinetic studies to evaluate the CNS penetration of this series (Table 9).

**Table 8.** Selected *in vitro* ADME properties assessment for chosen lead compounds.<sup>a</sup>

#	CID	SID	NCGC	SMN2 AC <sub>50</sub> (μM)	Rate of induction (%)	Luciferase inh. IC <sub>50</sub> (μM)	Mouse liver microsome T <sub>1/2</sub> (minute)	Caco-2 Permeability mean P <sub>app</sub> A → B (10 <sup>-6</sup> cm s <sup>-1</sup> )	Caco-2 Permeability mean P <sub>app</sub> B → A (10 <sup>-6</sup> cm s <sup>-1</sup> )
2	990823	87677807	NCGC00183533-01	1.22	268	inactive	12	30.7	12.1
6k	3292095	99367905	NCGC00183568-01	4.87	554	1.60	ND	32.6	12.0
9a	46907666	99367980	NCGC00187872-01	0.013	326	0.005	60	33.8	44.1
8m	46907676	99367992	NCGC00187898-01	0.031	576	40	2	1.6	0.2
9c	46907686	99367983	NCGC00187875-01	0.049	353	4.0	<15	ND	ND
8l	46907708	99367988	NCGC00187894-01	0.077	710	0.80	30	6.1	0.3
8c	46907733	99367986	NCGC00187892-01	0.077	609	6.4	7	ND	ND
8a	46907699	99367961	NCGC00187851-01	0.039	371	3.2	30	13.1	9.9
8b	46907746	99367991	NCGC00187897-01	0.122	257	3.2	60	21.2	51.2
7g	46907750	99367990	NCGC00187896-01	0.154	298	10	18	40.1	17.3

<sup>a</sup>Microsomal stability analysis was performed by Cerep and are based upon duplicate incubations of test reagent with mouse liver microsomes at 37 °C as described (www.cerep.com). LC/MS/MS is utilized to quantitate remaining test reagent. Test reagents were applied at standard concentrations (1 μM). Caco-2 permeability analysis was performed by Cerep as described (www.cerep.com). Data are expressed in P<sub>app</sub> (apparent permeability) in 10<sup>-6</sup> cm s<sup>-1</sup>. Colchicine and Ranitidine were used as a low permeability controls (Colchicine: mean A→B < 0.1 and mean B→A = 7.9; Ranitidine mean A→B = 0.2 and mean B→A = 2.8), Propranolol was used as a high permeability control (mean A→B = 41.0 and mean B→A = 39.4) and Labetalol was used as a P-gp substrate control (mean A→B = 7.3 and mean B→A = 36.6). Test reagents were applied at standard concentrations (10 μM).

### 3.6 Profiling Assays

N/A

### 3.7 *In vivo* Pharmacokinetic Assay

As we discussed in Section 3.5, the current probe **8m** had the liability of short half life in mouse liver microsomes; therefore, full pharmacokinetic analysis of another analog CID 46907708 (**8l**) was carried out to evaluate the CNS penetration. The plasma and brain concentration of CID 46907708 (**8l**) in male Swiss Albino Mice after single oral gavage administration of CID 46907708 (**8l**) at a dose of 30 mg/kg were measured. As data shown in Table 9, the plasma to brain ratio of CID 46907708 (**8l**) in male Swiss Albino Mice was found to be 0.29. CID 46907708 (**8l**) possessed a reasonable long half-life in brain ( $t_{1/2}$  = 5.44 h) as well as half-life in plasma ( $t_{1/2}$  = 5.78 h). The concentration of CID 46907708 (**8l**) in brain reached at 1.28 μmol/kg ( $C_{max}$ ) in only 5 minutes and maintained above the AC<sub>50</sub> concentration of 0.077 μM for more than 4 hours. In addition, no behavioral changes were observed in animals administered with test compound throughout the whole study period.

Oral administration of 30 mg/kg of <b>8l</b> in male Swiss Albino mice					
Mean plasma concentration			Brain concentration		
Sampling time (hr)	Mean (ng/mL)	Mean ( $\mu$ M)	Mean (ng/g)	Mean ( $\mu$ mol/kg)	
0	0	0	0	0	
0.083	1286	3.72	444	1.28	
0.25	416	1.2	109	0.31	
0.5	416	1.2	138	0.4	
1	439	1.27	207	0.6	
2	206	0.6	85	0.23	
4	0.98	0.0028	29	0.083	
8	8.49	0.025	0	0	
12	6.71	0.019	0	0	
24	20.64	0.06	7.78	0.023	

PK parameters	Unit	Estimate	PK parameters	Unit	Estimate
T <sub>max</sub>	hr	0.083	T <sub>max</sub>	hr	0.083
C <sub>max</sub>	ng/mL	1286 (3.72 $\mu$ M)	C <sub>max</sub>	ng/mL	444 (1.29 $\mu$ mol/kg)
T <sub>1/2</sub>	hr	5.78	T <sub>1/2</sub>	hr	5.44
AUC <sub>plasma</sub> (AUC <sub>last</sub> )	hr*ng/mL	1857	AUC <sub>plasma</sub> (AUC <sub>last</sub> )	hr*ng/mL	546
AUC <sub>INF</sub>	hr*ng/mL	1429	AUC <sub>INF</sub>	hr*ng/mL	607
AUC <sub>brain</sub> /AUC <sub>plasma</sub>	%	29			

**Table 9:** Pharmacokinetic Parameters for analog CID 46907708 (**8l**) following oral gavage administration to mice at 30 mg/kg.

## 4 Discussion

In summary, after several rounds of medicinal chemistry SAR studies, we were able to improve the potency of the hit compound by ~ 100 fold down to low double digit nanomolar AC<sub>50</sub>'s in our cell based luciferase reporter assay and also able to increase 3-7 fold of the rate of SMN protein production. From this study, analogs **8a** (AC<sub>50</sub> = 0.039  $\mu$ M, rate of induction = 370%), **8e** (AC<sub>50</sub> = 0.039  $\mu$ M, rate of induction = 550%), **8l** (AC<sub>50</sub> = 0.077  $\mu$ M, rate of induction = 709%), **8m** (the current 2<sup>nd</sup> probe, AC<sub>50</sub> = 0.031  $\mu$ M, rate of induction = 576%), **9a** (AC<sub>50</sub> = 0.012  $\mu$ M, rate of induction = 325%) were identified as novel SMN protein modulators. Analog **8m** was selected as the probe compound in consideration of the balance of potency, efficacy and selectivity. Though this probe compound **8m** had the liability of quick clearance, other analogs (**8l**, **9a**) in the series did show excellent stability in mouse liver microsomes. Therefore, this ADMET deficiency can be readily addressed by additional medicinal chemistry efforts. Additionally, compound **8l**, as a close analog of the probe compound **8m**, was showed good plasma-brain penetration and no side effects in the initial *in vivo* PK animal study.

As it was mentioned in the introduction, the severity of SMA correlated with the number of *SMN2* copies carried by the patient. In addition, SMN is ubiquitous and necessary for spliceosome assembly playing an important and fundamental role in the splicing machinery of every cell. The tissue specificity, triggering apoptosis mostly to motor neurons, indicates that small tissue variations in SMN production have a deep impact in the survival outcome. Experts in the field believe that it is necessary an up-regulation of SNM production of at least 20%, regarding the patient basal level, to have a therapeutic impact. Our best molecules clearly overpass that mark, increasing levels of production between 100 to 300% at low

nanomolar concentrations when they were tested in our primary reporter assay, as well as in meaningful orthogonal assays such as western blot and gems assays with patient fibroblasts. Moreover, one of our analogs showed good oral absorption and CNS penetration upon oral gavage administration at 30 mg/kg providing levels of exposure above its AC<sub>50</sub> for more than 4 h in brain, with no sign of toxicity or behavior disturbance in animals. For all these reasons, we consider this probe as an excellent candidate for advanced animal studies in SMA mouse models, and potentially for later development evaluating its capacity for becoming a SMA clinical candidate.

#### 4.1 Comparison to existing art and how the new probe is an improvement

As it had been previously mentioned in the introduction section, most of SMA drug candidates were repurposed bioactive agents, such as HDAC inhibitors, which had variety of liabilities including gastrointestinal bleeding, short half-life in human serum, high toxicity and lack of target specificity. In addition, the previously reported deCode compound from another qHTS campaign, D156844, was found inactive in our reporter assay. The current probe **8m** presented a novel chemotype with excellent *in vitro* activities in reporter assay, patient fibroblasts western blots and gem count assays. Furthermore, the initial *in vivo* PK animal study of its close analog **8l** showed good plasma-brain penetration and no side effects. We anticipate that the current series represented by the probe compound **8m** may serve as a useful probe for exploring the therapeutic benefits of SMN protein induction in SMA animal models, and ultimately in human clinical trials.

#### 4.2 Mechanism of Action Studies

As initial studies to have a better understanding of the mode of action, we decided to use RT-PCR to measure RNA expression levels and exon 7 inclusion within our reporter cell line (not endogenous SMN). Some analogs (**2**, **3f**, **9f**) showed a small increase in total SMN-luciferase transcripts but there was almost no increase in exon 7 mRNA (Data not shown). Although the mechanism of SMN protein induction by this class of arylpiperidine analogs was still unclear, this result indicated that SMN activity for this series might be post-transcriptional, potentially stabilizing SMN protein and somehow reducing its degradation.<sup>1</sup>

#### 4.3 Planned Future Studies

There will be three future directions for this project:

1. Move the current probe CID 46907676/ML200 (**8m**) or its analogs forward to animal study as the prove-of-concept for treatment of SMA in mice. Additional medicinal chemistry efforts are required to address the ADMET liability of the current compound. More pharmacokinetic studies at different doses need to be done. The long term study in the daily diets for SMA mice will require the scale up synthesis of the probe compound up to 10 grams.
2. Continue to explore additional SAR on the backup pyrimidine and thiodiazole series.
3. Develop additional cell based assay using a different reporter, such as Renila, to permanently eliminate the potential impact of luciferase inhibition in the reporter signal.

## 5 References

<sup>1</sup> (a) Roberts, D. F.; Chavez, J.; Court, S. D. The genetic component in child mortality. *Arch. Dis. Child.*, **1970**, *45*, 33-38. (b) Crawford, T. O.; Pardo, C. A. The neurobiology of childhood spinal muscular atrophy. *Neurobiol. Dis.*, **1996**, *3*, 97-110.

<sup>1</sup> Pearn, J. Incidence, prevalence, and gene frequency studies of chronic childhood spinal muscular atrophy. *J. Med. Genet.* **1978**, *15*, 409-413.

<sup>1</sup> (a) www.fsma.org. (b) Pearn, J. Classification of spinal muscular atrophies. *Lancet*, **1980**, *1*, 919-922.

<sup>1</sup> Lefebvre, S.; Burglen, L.; Reboullet, S.; Clermont, O.; Burlet, P.; Viollet, L.; Benichou, B.; Cruaud, C.; Millasseau, P.; Zeviani, M.; Le Paslier, D.; Frezal, J.; Cohen, D.; Weissenbach, J.; Munnich, A.; Melki, J. Identification and characterization of a spinal muscular atrophy-determining gene. *Cell*, **1995**, *80*, 155-165.

<sup>1</sup> Young, P. J.; Le, T. T.; Thi Man, N.; Burghes, A. H. M.; Morris, G. E. The relationship between SMN, the spinal muscular atrophy protein, and nuclear coiled bodies in differentiated tissues and cultured cells. *Exp. Cell Res.*, **2000**, *25*, 365-374.

<sup>1</sup> Lefebvre, S.; Burlet, P.; Liu, Q.; Bertrand, S.; Clermont, O.; Munnich, A.; Dreyfuss, G.; Melki, J. Correlation between severity and SMN protein level in spinal muscular atrophy. *Nat. Genet.*, **1997**, *16*, 265-269.

<sup>1</sup> Pellizzoni, L.; Baccon, J.; Charroux, B.; Dreyfuss, G. The survival of motor neurons (SMN) protein interacts with the snoRNP proteins fibrillarin and GAR1. *Current Biology*, **2001**, *11*, 1079-1088.

<sup>1</sup> (a) Lorson, C. L.; Hahnen, E.; Androphy, E. J.; Wirth, B. A single nucleotide in the SMN gene regulates splicing and is responsible for spinal muscular atrophy. *Proc. Natl. Acad. Sci. U.S.A.*, **1999**, *96*, 6307-6311. (b) Monani, U. R.; Lorson, C. L.; Parsons, D. W.; Prior, T. W.; Androphy, E. J.; Burghes, A. H. M.; McPherson, J. D. A single nucleotide difference that alters splicing patterns distinguishes the SMA gene *SMN1* from the copy gene *SMN2*. *Hum. Mol. Genet.* **1999**, *8*, 1177-1183.

<sup>1</sup> Lorson, C. L.; Strasswimmer, J.; Yao, J. M.; Baleja, J. D.; Hahnen, E.; Wirth, B.; Le, T. T.; Burghes, A. H. M.; Androphy, E. J. SMN oligomerization defect correlates with spinal muscular atrophy severity. *Nat. Genet.*, **1998**, *19*, 63-66.

<sup>1</sup> (a) Feldkotter, M.; Schwarzer, V.; Wirth, R.; Wienker, T. F.; Wirth, B. Quantitative analyses of *SMN1* and *SMN2* based on real-time light Cycler PCR: fast and highly reliable carrier testing and prediction of severity of spinal muscular atrophy. *Am. J. Hum. Genet.*, **2002**, *70*, 358-368. (b) McAndrew, P. E.; Parsons, D. W.; Simard, L. R.; Rochette, C.; Ray, P. N.; Mendell, J. R.; Prior, T. W.; Burghes, A. H. M. Identification of proximal spinal muscular atrophy carriers and patients by analysis of SMNT and SMNC gene copy number. *Am. J. Hum. Genet.*, **1997**, *60*, 1411-1422.

<sup>1</sup> Foust, K. D.; Wang, X.; McGovern, V. L.; Braun, L.; Bevan, A. K.; Haidet, A. M.; Le, T. T.; Morales, P. R.; Rich, M. M.; Burghes, A. H. M.; Kaspar, B. K. Rescue of the spinal muscular atrophy phenotype in a mouse model by early postnatal delivery of SMN. *Nat. Biotech.*, **2010**, *28*, 271–274.

<sup>1</sup> Hua, Y.; Sahashi, K.; Hung, G.; Rigo, F.; Passini, M. A.; Bennett, C. F.; Krainer, A. R. Antisense correction of *SMN2* splicing in the CNS rescues necrosis in a type III SMA mouse model. *Genes Dev.*, **2010**, *ASAP*.

<sup>1</sup> Deshpande, D. M.; Kim, Y. S.; Martinez, T.; Carmen, J.; Dike, S.; Shats, I.; Rubin, L. L.; Drummond, J.; Krishnan, C.; Hoke, A.; Maragakis, N.; Shefner, J.; Rothstein, J. D.; Kerr, D. A. Recovery from paralysis in adult rats using embryonic stem cells. *Ann. Neurol.*, **2006**, *60*, 32–44.

<sup>1</sup> Lunn, M. R.; Stockwell, B. R. Chemical genetics and orphan genetic diseases. *Chem. Biol.*, **2005**, *12*, 1063–1073.

<sup>1</sup> Chang, J.-G.; Hsieh-Li, H.-M.; Jong, Y.-J.; Wang, N. M.; Tsai, C.-H.; Li, H. Treatment of spinal muscular atrophy by sodium butyrate. *Proc. Natl. Acad. Sci. U.S.A.*, **2001**, *98*, 9808–9813.

<sup>1</sup> Andreassi, C.; Angelozzi, C.; Tiziano, F. D.; Vitali, T.; Vincenzi, E. D.; Boninsegna, A.; Villanova, M.; Bertini, E.; Pini, A.; Neri, G.; Brahe, C. Phenylbutyrate increases SMN expression *in vitro*: relevance for treatment of spinal muscular atrophy. *Eur. J. Hum. Genet.*, **2004**, *12*, 59–65.

<sup>1</sup> Grzeschik, S. M.; Ganta, M.; Prior, T. W.; Heavlin, W. D.; Wang, C. H. Hydroxyurea enhances *SMN2* gene expression in spinal muscular atrophy cells. *Ann. Neurol.*, **2005**, *58*, 194–202.

<sup>1</sup> Wirth, B.; Riessland, M.; Hahnen, E. Drug discovery for spinal muscular atrophy. *Expert Opin. Drug Discov.*, **2007**, *2*, 437–451.

<sup>1</sup> (a) Brichta, L.; Hofmann, Y.; Hahnen, E.; Siebzehnruhl, F. A.; Raschke, H.; Blumcke, I.; Eyupoglu, I. Y.; Wirth, B. Valproic acid increases the *SMN2* protein level: a well-known drug as a potential therapy for spinal muscular atrophy. *Hum. Mol. Genet.*, **2003**, *12*, 2481–2489. 32. (b) Sumner, C. J.; Huynh, T. N.; Markowitz, J. A.; Perhac, J. S.; Hill, B.; Coovert, D. D.; Schussler, K.; Chen, X.; Jarecki, J.; Burghes, A. H. M.; Taylor, J. P.; Fischbeck, K. H. Valproic acid increases SMN levels in spinal muscular atrophy patient cells. *Ann. Neurol.*, **2003**, *54*, 647–654.

<sup>1</sup> Andreassi, C.; Jarecki, J.; Zhou, J.; Coovert, D. D.; Monani, U. R.; Chen, X.; Whitney, M.; Pollok, B.; Zhang, M.; Androphy, E. J.; Burghes, A. H. M. Aclarubicin treatment restores SMN levels to cells derived from type I spinal muscular atrophy patients. *Hum. Mol. Genet.*, **2001**, *10*, 2841–2849.

<sup>1</sup> Wolstencroft, E. C.; Mattis, V.; Bajer, A. A.; Young, P. J.; Lorson, C. L. A non-sequence-specific requirement for SMN protein activity: the role of aminoglycosides in inducing elevated SMN protein levels. *Hum. Mol. Genet.*, **2005**, *14*, 1199–1210.

<sup>1</sup> Avila, A. M.; Burnett, B. G.; Taye, A. A.; Gabanella, F.; Knight, M. A.; Hartenstein, P.; Cizman, Z.; Di Prospero, N. A.; Pellizzoni, L.; Fischbeck, K. H.; Sumner, C. J. Trichostatin A increases SMN

expression and survival in a mouse model of spinal muscular atrophy. *J. Clin. Invest.*, **2007**, *117*, 659-671.

<sup>1</sup> (a) Hahnen, E.; Eyupoglu, I. Y.; Brichta, L.; Haastert, K.; Trankle, C.; Siebzehrubl, F. A.; Riessland, M.; Holker, I.; Claus, P.; Romstock, J.; et al. In vitro and ex vivo evaluation of second-generation histone deacetylase inhibitors for the treatment of spinal muscular atrophy. *J. Neurochem.*, **2006**, *98*, 193–202. (b) Riessland, M.; Ackermann, B.; Förster, A.; Jakubik, M.; Hauke, J.; Garbes, L.; Fritzsche, I.; Mende, Y.; Blumcke, I.; Hahnen, E.; Wirth, B. SAHA ameliorates the SMA phenotype in two mouse models for spinal muscular atrophy. *Hum. Mol. Genet.*, **2010**, *19*, 1492-1506.

<sup>1</sup> Yuo, C.-Y.; Lin, H.-H.; Chang, Y.-S.; Yang, W.-K.; Chang, J.-G. 5-(*N*-ethyl-*N*-isopropyl)-amiloride enhances *SMN2* exon 7 inclusion and protein expression in spinal muscular atrophy cells. *Ann. Neurol.*, **2008**, *63*, 26–34.

<sup>1</sup> **Garbes, L.; Riessland, M.; Hölker, I.; Heller, R.; Hauke, J.; Tränkle, C.; Coras, R.; Blümcke, I.; Hahnen, E.; Wirth, B.** LBH589 induces up to 10-fold SMN protein levels by several independent mechanisms **and** is effective even in cells from SMA patients non-responsive to valproate. *Hum. Mol. Genet.*, **2009**, *18*, 3645-3658.

<sup>1</sup> Dayangaç-Erden, D.; Bora, G.; Ayhan, P.; Kocaefe, C.; Dalkara, S.; Yelekçi, K.; Demir, A. S. Erdem-Yurter, H. Histone deacetylase inhibition activity and molecular docking of (*E*)-Resveratrol: its therapeutic potential in spinal muscular atrophy. *Chem. Biol. Drug Design*, **2009**, *73*, 355-364.

<sup>1</sup> Lunn, M. R.; Root, D. E.; Martino, A. M.; Flaherty, S. P.; Kelley, B. P.; Coover, D. D.; Burghes, A. H. M.; thi Man, N.; Morris, G. E.; Zhou, J.; Androphy, E. J.; Sumner, C. J.; Stockwell, B. R. Indoprofen upregulates the survival motor neuron protein through a cyclooxygenase-independent mechanism. *Chem. Biol.*, **2004**, *11*, 1489-1493.

<sup>1</sup> Hastings, M. L.; Berniac, J.; Liu, Y. H.; Abato, P.; Jodelka, F. M.; Barthel, L.; Kumar, S.; Dudley, C.; Nelson, M.; Larson, K.; Edmonds, J.; Bowser, T.; Draper, M.; Higgins, P.; Krainer, A. R. Tetracyclines that promote *SMN2* exon 7 splicing as therapeutics for spinal muscular atrophy. *Sci. Transl. Med.*, **2009**, *1*, 5ra12.

<sup>1</sup> Jarecki, J.; Chen, X.; Bernardino, A.; Coover, D. D.; Whitney, M.; Burghes, A. H. M.; Stack, J.; Pollok, B. A. Diverse small-molecule modulators of SMN expression found by high-throughput compound screening: early leads towards a therapeutic for spinal muscular atrophy. *Hum. Mol. Genet.*, **2005**, *14*, 2003-2018.

<sup>1</sup> (a) Thurmond, J.; Butchbach, M. E.; Palomo, M.; Pease, B.; Rao, M.; Bedell, L.; Keyvan, M.; Pai, G.; Mishra, R.; Haraldsson, M.; Andresson, T.; Bragason, G.; Thosteinsdottir, M.; Bjornsson, J. M.; Coover, D. D.; Burghes, A. H. M.; Gurney, M. E.; Singh, J. Synthesis and biological evaluation of novel 2,4-diaminoquinazoline derivatives as *SMN2* promoter activators for the potential treatment of spinal muscular atrophy. *J. Med. Chem.*, **2008**, *51*, 449-469. (b) Singh, J.; Salcius, M.; Liu, S. W.; Staker, B. L.; Mishra, R.; Thurmond, J.; Michaud, G.; Mattoon, D. R.; Printen, J.; Christensen, J.; Bjornsson, J. M.; Pollok, B. A.; Kiledjian, M.; Stewart, L.; Jarecki, J.; Gurney, M. E. DcpS as a therapeutic target for spinal muscular atrophy. *ACS Chem. Biol.*, **2008**, *3*, 711-722.

<sup>1</sup> Butchbach, M. E.; Singh, J.; Thornorsteinsdóttir, M.; Saieva, L.; Slominski, E.; Thurmond, J.; Andrésson, T.; Zhang, J.; Edwards, J. D.; Simard, L. R.; Pellizzoni, L.; Jarecki, J.; Burghes, A. H. M.; Gurney, M. E. Effects of 2,4-diaminoquinazoline derivatives on SMN expression and phenotype in a mouse model for spinal muscular atrophy. *Hum. Mol. Genet.*, **2009**, *19*, 454-467.

<sup>1</sup> *Chemical & Engineering News*, April 26, **2010**.

<sup>1</sup> It is interesting to find that <sup>both</sup> D156844 and another analogue **5g** <sup>in reference 30a</sup> were not active in our **current** <sup>in-</sup>house luciferase reporter assay.

<sup>1</sup> Nicolaou, K. C.; He, Y.; Roschangar, F.; King, N. P.; Vourloumis, D.; Li, T. Total synthesis of epothilone E & analogs with modified side chains through the Stille coupling reaction. *Angew. Chem., Int. Ed. Engl.*, **1998**, *37*, 84-87.

<sup>1</sup> Miyaura, N.; Suzuki, A. Palladium-catalyzed cross-coupling reactions of organoboron compounds. *Chem. Rev.*, **1995**, *95*, 2457-2483.

<sup>1</sup> Jolidon, S.; Narquizian, R.; Norcross, R. D.; Pinard, E. [4-(Heteroaryl) piperazin-1-yl]-(2,5-substituted-phenyl)methanone derivatives as glycine transporter 1 (glyt-1) inhibitors for the treatment of neurological and neuropsychiatric disorders. *PCT Patent Application: WO2006/72436 A1*, **2006**.

<sup>1</sup> Palani, A.; Berlin, M. Y.; Aslanian, R. G.; Vaccaro, H. M.; Chan, T.-Y.; Xiao, D.; Degrado, S.; Rao, A. U.; Chen, X.; Lee, Y. J.; Sofolarides, M. J.; Shao, N.; Huang, Y. R.; Liu, Z.; Wang, L. Y.; Pu, H. Pyrrolidine, piperidine and piperazine derivatives and methods of use thereof. *PCT Patent Application: WO2010/45303 A2*, **2010**.

<sup>1</sup> Plant, A.; Seitz, T.; Jansen, J. R.; Erdelen, C.; Turberg, A.; Hansen, O. Delta 1-pyrrolines used as pesticides. *U.S. Patent Application: US2004/82586 A1*, **2004**.

<sup>1</sup> Sekiguchi, Y.; Kanuma, K.; Omodera, K.; Tran, T.-A.; Semple, G.; Kramer, B. A. Pyrimidine derivatives and methods of treatment related to the use thereof. *PCT Patent Application: WO/2005/095357*, **2005**.

<sup>1</sup> Westhuyzen, C. W. van der; Rousseau, A. L.; Parkinson, C. J. Effect of substituent structure on pyrimidine electrophilic substitution. *Tetrahedron*, **2007**, *63*, 5394-5405.

<sup>1</sup> Devasagayaraj, A.; Jin, H.; Liu, Q.; Marinelli, B.; Samala, L.; Shi, Z.-C.; Tunoori, A.; Wang, Y.; Wu, W.; Zhang, C.; Zhang, H. Multicyclic amino acid derivatives and methods of their use. *U.S. Patent Application: US2007/191370 A1*, **2007**.

<sup>1</sup> Zhang, M. L.; Lorson, C. L.; Androphy, E. J.; Zhou, J. An *in vivo* reporter system for measuring increased inclusion of exon 7 in *SMN2* mRNA: potential therapy of SMA. *Gene Therapy*, **2001**, *8*, 1532-1538.



<sup>1</sup> Inglese, J.; Auld, D. S.; Jadhav, A.; Johnson, R. L.; Simeonov, A.; Yasgar, A.; Zheng, W.; Austin, C. P. Quantitative high-throughput screening: A titration-based approach that efficiently identifies biological activities in large chemical libraries. *Proc. Natl. Acad. Sci. U.S.A.*, **2006**, *103*, 11473–11478.

<sup>1</sup> Austin, C. P.; Brady, L. S.; Insel, T. R.; Collins, F. S. NIH molecular libraries initiative. *Science* **2004**, *306*, 1138-1139.

<sup>1</sup> (a) Auld, D. S.; Zhang, Y. Q.; Southall, N. T.; Rai, G.; Landsman, M.; Maclure, J.; Langevin, D.; Thomas, C. J.; Austin, C. P.; Inglese, J. A basis for reduced chemical library inhibition of firefly luciferase obtained from directed evolution. *J. Med. Chem.*, **2009**, *52*, 1450-1458. (b) Auld, D. S.; Thorne, N.; Nguyen, D.-T.; Inglese, J. A specific mechanism for nonspecific activation in reporter-gene assays. *ACS Chem. Bio.*, **2008**, *3*, 463-470. (c) Auld, D. S.; Thorne, N.; Maguire, W. F.; Inglese, J. Mechanism of PTC124 activity in cell-based luciferase assays of nonsense codon suppression. *Proc. Natl. Acad. Sci. U.S.A.*, **2009**, *106*, 3585–3590.

<sup>1</sup> Xia, M.; Huang, R.; Guo, V.; Southall, N.; Cho, M.-H.; Inglese, J.; Austin, C. P.; Nirenberg, M. Identification of compounds that potentiate CREB signaling as possible enhancers of long-term memory. *Proc. Natl. Acad. Sci. U.S.A.*, **2009**, *106*, 2412-2417.

<sup>1</sup> van Breemen, R. B.; Li, Y. Caco-2 cell permeability assays to measure drug absorption. *Expert Opin. Drug Metab. Toxicol.*, **2005**, *1*, 175-185.

<sup>1</sup> Aller, S. G.; Yu, J.; Ward, A.; Weng, Y.; Chittaboina, S.; Zhuo, R.; Harrell, P. M.; Trinh, Y. T.; Zhang, Q.; Urbatsch, I. L.; Chang, G. Structure of P-glycoprotein reveals a molecular basis for poly-specific drug binding. *Science*, **2009**, *323*, 1718–1722.

<sup>1</sup> Coover, D. D.; Le, T. T.; McAndrew, P. E.; Strasswimmer, J.; Crawford, T. O.; Mendell, J. R.; Coulson, S. E.; Androphy, E. J.; Prior, T. W.; Burghes, A. H. M. The survival motor neuron protein in spinal muscular atrophy. *Hum. Mol. Genet.* **1997**, *6*, 1205-1214.

<sup>1</sup> We have seen this pattern previously with LDDN hits (unpublished results from the laboratory of Elliot J. Androphy).

**Probe Report**

**Title:** Identification of SMN modulators for potential SMA disease therapeutics

**Authors:** Elliott Androphy, Wei Zheng, Steve Titus, Jonathan Cherry, Jingbo Xiao, Juan Marugan, Noel Southall, Christopher Austin

**Assigned Assay Grant #:** MH084179-01

**Screening Center Name & PI:** NCGC & Christopher P. Austin

**Chemistry Center Name & PI:** NCGC & Christopher P. Austin

**Assay Submitter & Institution:** Elliot Androphy, University of Massachusetts Medical School

**PubChem Summary Bioassay Identifier (AID):** 1474

**Probe Structure & Characteristics:**

**PubChem CID:** 990823

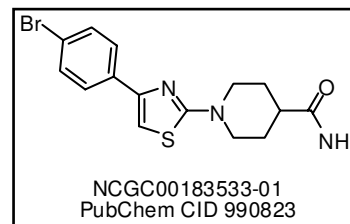
**Internal ID:** NCGC00183533-01

**IUPAC Name:** 1-(4-(4-bromophenyl)thiazol-2-yl)

piperidine-4-carboxamide

**Chemical Formula:** C<sub>15</sub>H<sub>16</sub>BrN<sub>3</sub>OS

**Exact Mass:** 365.0197



CID**	Target Name <sup>‡</sup>	IC50/EC50 (nM) [SID, AID] <sup>†</sup>	Anti-target Name(s) <sup>‡</sup>	IC50/EC50 (μM) [SID, AID] <sup>†</sup>	Select-ivity*	Secondary Assay(s)  Name: IC50/EC50 (nM) [SID,

						<b>AID]<sup>§</sup></b>
990823	Survival motor neuron 2 Protein expression	770 nM [87677807, 1740]	SMN1 protein expression, Luciferase inhibition	77 uM [87677807, 1739], 40 uM [87677807, 1733]	50 to 100-fold	Western Blot of SMN protein in patient fibroblasts: 100 nM [87677807, 1474]

‡Short descriptive name of target or pathway (similar for antitarget, if applicable).

†IC<sub>50</sub>/EC<sub>50</sub> value in nM along with the PubChem SID and AID where this value can be found.

§For secondary assay provide the following information: Name, IC<sub>50</sub>/EC<sub>50</sub> [SID, AID]

\*Selectivity = antitarget IC<sub>50</sub>/target IC<sub>50</sub>

\*\*Provide the PubChem CID for the probe.

### Recommendations for the scientific use of this probe:

This is the second probe report for SMN with a different chemotype and more reasonable SAR. This probe should be useful for increasing the expression of SMN protein in cell-based models of SMN2 expression. This probe has not been evaluated for use *in vivo*, though it has been shown to increase SMN2 protein production in fibroblasts derived from SMA patients. This compound may alter SMN2 gene splicing, but mode of action studies are still under investigation. The goal of the project was to identify a compound with 10-fold selectivity for SMN2 versus SMN1 expression in reporter based assays that increase SMN protein abundance in primary SMA patient derived fibroblasts. CID 990823 satisfies these criteria, increasing protein expression in fibroblasts derived from SMA patients using Western Blot analysis at a compound concentration of 100 nM, and was one of the most potent members of the series in the primary screening assay.

## **Biological activity of this probe in comparison to other literature compounds:**

Several small molecule compounds were previously identified that increase SMN transcript and/or protein levels in SMA patient-derived cell lines. However, their activities appear to be distinct from the present series. Sodium butyrate, aclarubicin and valproic acid all non-specifically enhance reporter response from both the SMN1 and SMN2 loci in addition to having significant liabilities (short half-life, side effects, toxicity et al.) (Lunn, et al. 2005). Lunn et al. 2004 identified indoprofen as having an effect on full length SMN2 expression in a cell-based reporter assay, but also non-specifically enhances reporter response and it is not very potent ( $> 1 \mu\text{M}$ ). Other previous screens identified other HDAC inhibitors and one novel chemical series (described in Jarecki, et al. 2005) that can modulate reporter activity. The latter's molecular target appears to be DcpS, which modulates SMN2 protein levels by stabilizing the SMN2 mRNA transcript (Singh, et al. 2008). Though D156844 showed early promise in the animal study, it has not been shown whether D156844 acts specifically on SMN2 mRNA transcript stability; regardless D156844 was inactive in the present SMN2 reporter assay.

The present probe is potent (770 nM) and specifically affects expression of SMN2 indicating distinct mechanism of action from previously reported compounds. This chemotype is an improvement over the previously reported probe in that it possesses both a more tractable SAR and more drug-like physical properties.

### **1. Scientific rationale for project**

Spinal muscular atrophy (SMA) is caused by insufficient levels of the survival motor neuron (SMN) protein. The SMN locus on chromosome 5q13 contains two inverted copies, SMN1 and SMN2, which are 99% identical at the amino acid level. At the

splicing level, SMN1 produces mainly one splice variant (90%) containing exons 1-8 identified as SMN protein, which is the fully functional protein. Protein from SMN2 expression excludes exon 7 ~90% of the time. Skipping of exon 7 produces an unstable SMN protein that is rapidly degraded. In the SMA disease state, various mutations in the SMN1 locus render protein expressed from that locus nonfunctional and induce the disease state. The 10% of SMN2 protein expression that is correctly spliced is not sufficient to overcome the deficiency produced by the loss of the SMN1 protein due to the genetic mutations. Therefore, increasing overall SMN production through upregulation of *SMN2* promoter or through the modulation of the splicing to include the exon-7 by a small molecule modulator has been postulated as one of the potential therapeutic strategies for SMA.

We have designed and performed a cell based luciferase reporter gene assay by combining the promoter and splicing based cassettes in tandem with the major portion of the native SMN2 cDNA. A screen of this assay with a compound library can identify compounds that increase SMN2 levels by three mechanisms: modulating alternative splicing of SMN exon 7, increasing transcription from the SMN2 promoter, or stabilizing the SMN protein. Earlier screening assays for SMA only targeted compounds that either stimulate the SMN2 promoter or decrease exon 7 skipping.

## **Project description**

### **Original goal for probe**

To identify small molecules which increase the level of SMN transcript harboring the full length of SMN protein. This could be due to modulation of splicing, by increasing the level of transcript produced or stabilizing the SMN protein.

Over the past several years, several small molecule compounds have been identified that increase SMN transcript and/or protein levels in SMA patient-derived cell lines. These include the short chain fatty acid butyrate, aclarubicin and valproic acid, but all have significant liabilities (Lunn, et al. 2005). Lunn et al. 2004 identified indoprofen as having an effect on full length SMN2 expression in a cell-based reporter assay, but is was not potent ( $>1\mu\text{M}$ ) and increased protein expression by only 13% (p-value  $<0.0139$ ). Other previous screens identified other HDAC inhibitors and two novel chemical series (described in Jarecki, et al. 2005 as Compound A, G1 and G2) that can modulate reporter activity in the reporter cell line (Figure 1).

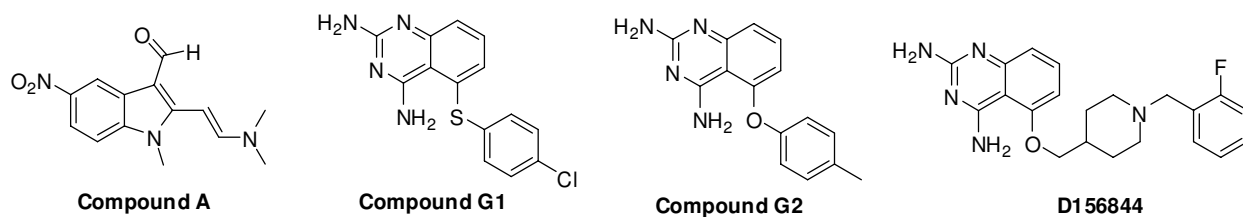


**Figure 1.** Structures of Compound A (CID 867234), G1 (CID 462589), G2 (CID 4106338) and D156844 (CID 23729147).

During the processing of this RO3 application, Compound G's SAR has been further developed, and its molecular target identified. The current probe from that series is identified as D156844 (Thurmond, et al. 2008); its molecular target appears to be DcpS, which modulates SMN2 protein levels by stabilizing the SMN2 mRNA transcript (Singh, et al. 2008). It has not been shown whether D156844 acts specifically on SMN2 mRNA transcript stability, but it was inactive in the present SMN-luciferase fusion reporter assay.

To date, we have identified and submitted one probe report identifying a separate chemotype that increases the level of SMN transcript harboring the full length of SMN protein. This first chemotype has a very narrow SAR. The present probe is for a new chemotype that possesses a more tractable SAR.

### Screens deposited to PubChem.

PubChem AID	Type	Target	Conc. Range	Samples Tested
<b>1458</b>	Primary qHTS	SMN-luc protein production from the SMN2 locus.	57.5 $\mu$ M – 0.7 nM	211,511

<b>1740</b>	Confirmatory	SMN-luc protein production from the SMN2 locus.	57.5 uM – 0.01 uM	117
<b>1739</b>	Anti-target	SMN-luc protein production from the SMN1 locus.	57.5 μM – 0.7 nM	117
<b>1733</b>	Anti-target	Luciferase enzymatic inhibition.	57.5 μM – 0.7 nM	110
<b>2514</b>	Confirmatory	SMN-luc protein production from the SMN2 locus.	57.5 uM – 0.01 uM	29
<b>2513</b>	Anti-target	SMN-luc protein production from the SMN1 locus.	57.5 μM – 0.7 nM	29
<b>2515</b>	Anti-target	Luciferase enzymatic inhibition.	57.5 μM – 0.7 nM	28
<b>1474</b>	Summary			

## **qHTS assay for high throughput screening for SMA [AID:1458]**

### **Assay details and protocol.**

#### **Center summary of the primary screen:**

This screen utilizes a luciferase reporter gene assay, combining the promoter and splicing based cassettes in tandem with the major portion of the native SMN2 cDNA, which was stably transfected into HEK293 cells. Compounds that increase



the SMN-luciferase reporter fusion signal presumably enhance expression of the functional SMN2 splice variant – the full length protein including exon-7.

*Assay protocol:*

Passaging media contained DMEM w/ glutamax (+phenol red) 10% FCS, 1x pen/strep, 200 ug/ml hygro, 1x sodium pyruvate. Assay media contained DMEM w/ glutamax (-phenol red) 10% FCS, 1x pen strep, 1x pyruvate

Sequence, Parameter, Value, Description

- (1) Cells, 5 uL, 2000 cells/well, 1536 TC treated White solid bottom plate
- (2) Time, 10-12 hours, 37C 5% CO2
- (3) Compound, 23 nl, MLSMR Library
- (4) Control Compound, 23 nL, Sodium butyrate st 4.5mM (final) conc
- (5) Time, 30-36 hours, 37C 5% CO2
- (6) Reagent, 3 ul, OneGlo (TM) from Promega
- (7) Time, 5-15 minutes, Room temp
- (8) Detector, Viewlux: luminescent read, 60 second integration, high speed 2x binning

**Primary assay summary**

211,000 compounds were screened in 1229 1536-well plates over 5 days on the robotic system (1,887,744 wells). Signal-to-background averaged 9-fold and Z' was

0.53. There were many potent hits in this screen, however many of these compounds were known to potently inhibit luciferase.

### Identification of lead

The vast majority of hits in the primary screen were luciferase inhibitors which presumably stabilized the SMN-luciferase fusion protein and prevented cellular degradation – though this has not been explicitly proven. Because of this, active compounds covering a diverse selection of chemotypes, some known to inhibit luciferase, others not, were chosen for further characterization.

### Confirmatory assay

This diverse set of chemotypes were sent out for confirmation in the assay provider's lab in the luciferase-based reporter assay as well as in a (luciferase-free) SMA-derived patient fibroblast assay for SMN protein production by Western Blot. CID 990823 increased SMN protein production in this assay (Figure 1).

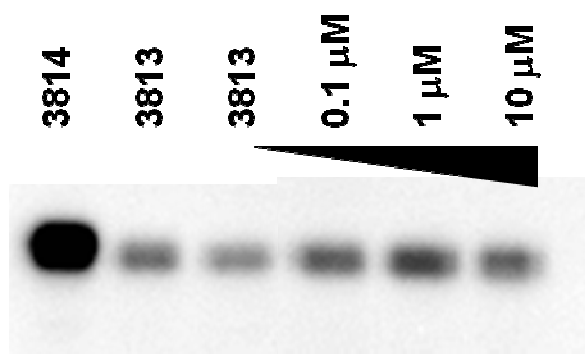


**Figure 1.** CID 990823 effect on SMN protein production in SMA patient derived fibroblasts (labeled 3813). CID 990823 was tested at three concentrations and incubated with cells for 40 hours. A control fibroblast cell type (labeled 3814) shows endogenous SMN protein production.

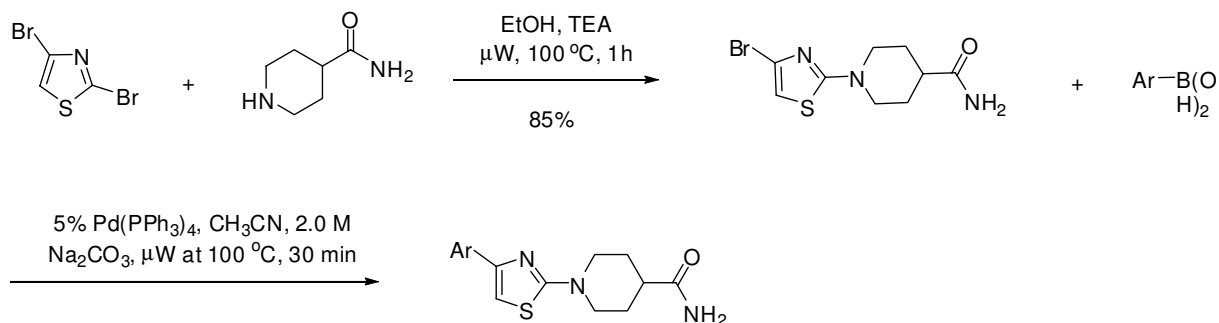
### **Anti-target assay(s)**

CID 990823 and other compounds were assayed for luciferase inhibition and SMN-luciferase fusion protein production from the SMN1 locus. Some modest activity was observed in these assays, but with a 100-fold selectivity. These assays were then utilized to examine the activity of CID 990823 and all related analogs.

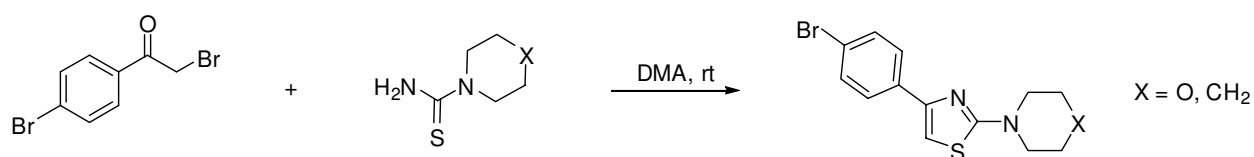
### **Synthesis of the probe CID 990823 and its analogues**

We developed a convergent approach toward the synthesis of the probe (CID 990823) and its closely related analogues as detailed in Scheme 1. Specifically, selective amination of 2 position of 2,4-dibromothiazole provided the key building block 1-(4-bromothiazol-2-yl)piperidine-4-carboxamide. A straightforward Suzuki coupling of the said building block with various commercially available arylboronic acid or pinacol ester generated the desired products. The analogues with the modification of piperidine ring were synthesized via thiazole ring formation by  $\alpha$ -bromoketone and thiourea (Scheme 2). All final compounds were purified by preparative scale HPLC.

### **Scheme 1**



## Scheme 2

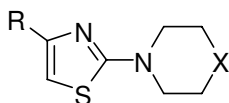


## Activity for CID 990823 and selected analogues.

Analogues of this chemotype were prepared including comprehensive variations on the aromatic ring and piperidine ring, and tested in the primary screening assay to establish potency and efficacy. Table 1 shows that most of the *ortho* substituents at the phenyl ring yield compounds less active both in AC<sub>50</sub> and efficacy, with the exception of the *ortho* fluoro substitution. This data indicates the potential necessity of having a co-planar conformation between the two aromatic rings for maintaining good activity. In general, electro-donating functional groups at *meta* or *para* position of the phenyl tend to provide better activity and efficacy than corresponding electro-withdrawing groups. Several aromatic substitutions increase the activity and/or maintain or increase the efficacy of the lead compound. For example, the *meta* *N,N*-dimethylamine substituent (NCGC00183564-01) and the *para* methyl substituent (NCGC00183582-01), reduce the AC<sub>50</sub> without diminishing the efficacy. As for the heteroaromatic rings, none of them had a positive impact

on the activity/efficacy of the molecule. We also study several polycyclic aromatic rings, however, most of them decrease the activity/efficacy, with the exception of the benzodioxane ring analogue (NCGC00183579-01) showing a trend of improvement in both the activity/efficacy which matched with the earlier stated positive electro-donating effect. The terminal amide bond is also found to be essential for the activity/efficacy (NCGC00183534-01 and NCGC00183536-01).

**Table 1.** Structures of the synthesized analogues and their SAR. While HDAC inhibitors and other compounds that non-specifically increase reporter expression increase expression at both SMN1 and SMN2 loci, the probe series actually inhibited SMN1 expression at higher concentrations of compound. Hence an IC<sub>50</sub> is reported for the SMN1 assay here.



PubChem CID	PubChem SID	Compound Internal Identifier	R	X	SMN2 AC <sub>50</sub> (μM)	SMN2 Max. Res (%)	SMN1 IC <sub>50</sub> (μM)	Luciferase IC <sub>50</sub> (μM)
44143946	87677806 85148605	NCGC00183531-01 (MLS002391463)	4-fluorophenyl	CHC(O)NH <sub>2</sub>	3.45	231	77.2	28.4
990823 (Probe)	87677807 22404505	NCGC00183533-01 (MLS000698854)	4-bromophenyl	CHC(O)NH <sub>2</sub>	0.77	377	77.2	40.1
720656	87677808 24808841	NCGC00183534-01 (MLS000710046)	4-bromophenyl	O	15.4	44	48.7	126.7
2900985	87677809	NCGC00183536-01	4-bromophenyl	CH <sub>2</sub>	13.7	187	>100	17.9
44143948	87677810	NCGC00183537-01	2-naphthalenyl	CHC(O)NH	4.87	170	>100	31.8

				2				
44144337	87677811	<i>NCGC00183540-01</i>	2-fluorophenyl	CHC(O)NH 2	1.37	166	>100	35.7
44144339	87677812 85149199	<i>NCGC00183543-01</i> <i>(MLS002391471)</i>	2-trifluoromethylphenyl	CHC(O)NH 2	>100		>100	>100
44144341	87677813 85149200	<i>NCGC00183544-01</i> <i>(MLS002391472)</i>	2-methylsulfonylphenyl	CHC(O)NH 2	>100		>100	>100
44144355	87677814	<i>NCGC00183546-01</i>	3-pyridin-yl	CHC(O)NH 2	>100		>100	>100
44144331	87677815	<i>NCGC00183548-01</i>	4-methoxyphenyl	CHC(O)NH 2	4.34	210	>100	89.7
44144333	87677816	<i>NCGC00183549-01</i>	2-bromophenyl	CHC(O)NH 2	>100		>100	80.0
44144351	87677817	<i>NCGC00183554-01</i>	(3,5-dimethyl)isoxazol-4-yl	CHC(O)NH 2	>100		>100	>100
44144353	87677818	<i>NCGC00183555-01</i>	2-aminoophenyl	CHC(O)NH 2	34.5	90	>100	>100
44144357	87677819	<i>NCGC00183556-01</i>	3-acetylphenyl	CHC(O)NH 2	3.87	437	>100	50.5
44144359	87677820	<i>NCGC00183557-01</i>	3-aminoophenyl	CHC(O)NH 2	>100		>100	>100
44144361	87677821	<i>NCGC00183559-01</i>	2-( <i>N,N</i> -dimethylamino)phenyl	CHC(O)NH 2	>100		>100	>100
44144367	87677822	<i>NCGC00183562-01</i>	1-methyl-1H-indol-5-yl	CHC(O)NH 2	4.34	367	>100	10.1
44143158	87677823	<i>NCGC00183563-01</i>	2-biphenyl	CHC(O)NH 2	>100		>100	89.7
44144365	87677824	<i>NCGC00183564-01</i>	3-( <i>N,N</i> -dimethylamino)phenyl	CHC(O)NH 2	0.69	388	48.7	12.7
44144363	87677825	<i>NCGC00183565-01</i>	3-(dimethylcarbamoyl)phenyl	CHC(O)NH 2	10.9	61	>100	>100
44144369	87677826	<i>NCGC00183567-01</i>	2-benzofuranyl	CHC(O)NH 2	8.67	102	>100	31.8
44144335	87677827	<i>NCGC00183571-01</i>	3-chlorophenyl	CHC(O)NH 2	12.2	59	>100	56.6
44143156	87677828	<i>NCGC00183573-01</i>	3-methylsulfonylphenyl	CHC(O)NH 2	>100		>100	>100
44144343	87677829	<i>NCGC00183575-01</i>	4-acetylphenyl	CHC(O)NH	7.72	130	>100	100.7

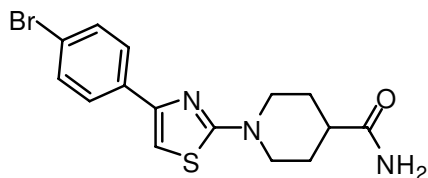
	85149201	(MLS002391474)		2				
44144345	87677830	NCGC00183579-01	2,3-dihydrobenzo[b][1,4]dioxin-6-yl	CHC(O)NH 2	0.69	397	19.4	4.50
44144347	87677831	NCGC00183580-01	4-oxo-4H-chromen-6-yl	CHC(O)NH 2	7.72	473	>100	63.5
44144349	87677832	NCGC00183581-01	2-thiophenyl	CHC(O)NH 2	7.72	70	>100	71.3
44143947	87677833	NCGC00183582-01	4-methylphenyl	CHC(O)NH 2	0.77	297	38.7	12.7

## Probe

### Chemical name of probe compound:

1-(4-(4-bromophenyl)thiazol-2-yl)piperidine-4-carboxamide

### Probe chemical structure including stereochemistry if known:



NCGC00183533-01

### Structural verification information of probe SID:

1-(4-(4-bromophenyl)thiazol-2-yl)piperidine-4-carboxamide (NCGC00183533-01).  
 $^1\text{H}$  NMR (400 MHz,  $\text{DMSO}-d_6$ )  $\delta$  7.83-7.79 (m, 2 H), 7.59-7.55 (m, 2 H), 7.33 (s, 1 H), 7.32 (br. s., 1 H), 6.82 (br. s., 1 H), 3.96 (br. d.,  $J=12.8$  Hz, 2 H), 3.06 (td,  $J=12.6, 2.9$  Hz, 2 H), 2.36 (tt,  $J=11.6, 3.8$  Hz, 1 H), 1.82 (dd,  $J=13.0, 2.6$  Hz, 2 H), 1.61 (qd,  $J=12.4, 4.0$  Hz, 2 H); LC/MS: retention time, 5.165 min,  $m/z$  366.0  $[\text{M}+\text{H}^+]$ .

### PubChem CID (corresponding to the SID):



990823

**If available from a vendor, please provide details:**

Ambinter Catalog# STK130838

**Provide MLS# that verifies the submission of probe molecules and five related samples that were submitted to the SMR collection:**

MLS000698854 (probe)

MLS002391463

MLS000710046

MLS002391471

MLS002391472

MLS002391474

**Describe mode of action for biological activity of probe:**

SMN protein expression modulator.

**Detailed Synthetic pathway for making probe:**

See above.

**Center summary of probe properties (solubility, absorbance/fluorescence, reactivity, toxicity, etc.):**

Compound is soluble at 10 mM in DMSO. Solubility in buffer has not been tested.

**A tabular presentation summarizing known probe properties:**

PubChem CID	990823
Molecular Weight	366.28
Molecular Formula	C <sub>15</sub> H <sub>16</sub> BrN <sub>3</sub> OS
CLogP	2.44591
H-Bond Donor	1
H-Bond Acceptor	4
Rotatable Bond Count	5
Exact Mass	365.02
Topological Polar Surface Area	58.69

**IUPAC Name:**

1-(4-(4-bromophenyl)thiazol-2-yl)piperidine-4-carboxamide

## Canonical SMILES:

O=C(N)C(CC1)CCN1C2=NC(C3=CC=C(Br)C=C3)=CS2

## Bibliography

1. Jarecki, J. et al. Diverse small-molecule modulators of SMN expression found by high-throughput compound screening: early leads towards a therapeutic for spinal muscular atrophy. *Hum Mol Genet* 14, 2003-2018 (2005).
2. Lunn, M.R. et al. Indoprofen upregulates the survival motor neuron protein through a cyclooxygenase-independent mechanism. *Chem Biol* 11, 1489-1493 (2004).
3. Thurmond, J. et al. Synthesis and biological evaluation of novel 2,4-diaminoquinazoline derivatives as SMN2 promoter activators for the potential treatment of spinal muscular atrophy. *J Med Chem* 51, 449-469 (2008).
4. Singh, J. et al. DcpS as a Therapeutic Target for Spinal Muscular Atrophy. *ACS Chem Biol* (2008).
5. Inglese, J. et al. Quantitative high-throughput screening: a titration-based approach that efficiently identifies biological activities in large chemical libraries. *Proc Natl Acad Sci U S A* 103, 11473-11478 (2006).

---

<sup>i</sup> (a) Roberts, D. F.; Chavez, J.; Court, S. D. The genetic component in child mortality. *Arch. Dis. Child.*, **1970**, *45*, 33-38. (b) Crawford, T. O.; Pardo, C. A. The neurobiology of childhood spinal muscular atrophy. *Neurobiol. Dis.*, **1996**, *3*, 97-110.

<sup>ii</sup> Pearn, J. Incidence, prevalence, and gene frequency studies of chronic childhood spinal muscular atrophy. *J. Med. Genet.* **1978**, *15*, 409-413.

<sup>iii</sup> (a) www.fsma.org. (b) Pearn, J. Classification of spinal muscular atrophies. *Lancet*, **1980**, *1*, 919-922.

<sup>iv</sup> Lefebvre, S.; Burglen, L.; Reboullet, S.; Clermont, O.; Burlet, P.; Viollet, L.; Benichou, B.; Cruaud, C.; Millasseau, P.; Zeviani, M.; Le Paslier, D.; Frezal, J.; Cohen, D.; Weissenbach, J.; Munnich, A.; Melki, J. Identification and characterization of a spinal muscular atrophy-determining gene. *Cell*, **1995**, *80*, 155-165.

<sup>v</sup> Young, P. J.; Le, T. T.; Thi Man, N.; Burghes, A. H. M.; Morris, G. E. The relationship between SMN, the spinal muscular atrophy protein, and nuclear coiled bodies in differentiated tissues and cultured cells. *Exp. Cell Res.*, **2000**, *25*, 365-374.

<sup>vi</sup> Lefebvre, S.; Burlet, P.; Liu, Q.; Bertrand, S.; Clermont, O.; Munnich, A.; Dreyfuss, G.; Melki, J. Correlation between severity and SMN protein level in spinal muscular atrophy. *Nat. Genet.*, **1997**, *16*, 265-269.

<sup>vii</sup> Pellizzoni, L.; Baccon, J.; Charroux, B.; Dreyfuss, G. The survival of motor neurons (SMN) protein interacts with the snoRNP proteins fibrillarin and GAR1. *Current Biology*, **2001**, *11*, 1079-1088.

<sup>viii</sup> (a) Lorson, C. L.; Hahnen, E.; Androphy, E. J.; Wirth, B. A single nucleotide in the SMN gene regulates splicing and is responsible for spinal muscular atrophy. *Proc. Natl. Acad. Sci. U.S.A.*, **1999**, *96*, 6307-6311. (b) Monani, U. R.; Lorson, C. L.; Parsons, D. W.; Prior, T. W.; Androphy, E. J.; Burghes, A. H. M.; McPherson, J. D. A single nucleotide difference that alters splicing patterns distinguishes the SMA gene *SMN1* from the copy gene *SMN2*. *Hum. Mol. Genet.* **1999**, *8*, 1177-1183.

<sup>ix</sup> Lorson, C. L.; Strasswimmer, J.; Yao, J. M.; Baleja, J. D.; Hahnen, E.; Wirth, B.; Le, T. T.; Burghes, A. H. M.; Androphy, E. J. SMN oligomerization defect correlates with spinal muscular atrophy severity. *Nat. Genet.*, **1998**, *19*, 63-66.

<sup>x</sup> (a) Feldkotter, M.; Schwarzer, V.; Wirth, R.; Wienker, T. F.; Wirth, B. Quantitative analyses of *SMN1* and *SMN2* based on real-time light Cycler PCR: fast and highly reliable carrier testing and prediction of severity of spinal muscular atrophy. *Am. J. Hum. Genet.*, **2002**, *70*, 358-368. (b) McAndrew, P. E.; Parsons, D. W.; Simard, L. R.; Rochette, C.; Ray, P. N.; Mendell, J. R.; Prior, T. W.; Burghes, A. H. M. Identification of proximal spinal muscular atrophy carriers and patients by analysis of SMN1 and SMN2 gene copy number. *Am. J. Hum. Genet.*, **1997**, *60*, 1411-1422.

---

<sup>xi</sup> Foust, K. D.; Wang, X.; McGovern, V. L.; Braun, L.; Bevan, A. K.; Haidet, A. M.; Le, T. T.; Morales, P. R.; Rich, M. M.; Burghes, A. H. M.; Kaspar, B. K. Rescue of the spinal muscular atrophy phenotype in a mouse model by early postnatal delivery of SMN. *Nat. Biotech.*, **2010**, *28*, 271–274.

<sup>xii</sup> Hua, Y.; Sahashi, K.; Hung, G.; Rigo, F.; Passini, M. A.; Bennett, C. F.; Krainer, A. R. Antisense correction of *SMN2* splicing in the CNS rescues necrosis in a type III SMA mouse model. *Genes Dev.*, **2010**, *ASAP*.

<sup>xiii</sup> Deshpande, D. M.; Kim, Y. S.; Martinez, T.; Carmen, J.; Dike, S.; Shats, I.; Rubin, L. L.; Drummond, J.; Krishnan, C.; Hoke, A.; Maragakis, N.; Shefner, J.; Rothstein, J. D.; Kerr, D. A. Recovery from paralysis in adult rats using embryonic stem cells. *Ann. Neurol.*, **2006**, *60*, 32-44.

<sup>xiv</sup> Lunn, M. R.; Stockwell, B. R. Chemical genetics and orphan genetic diseases. *Chem. Biol.*, **2005**, *12*, 1063-1073.

<sup>xv</sup> Chang, J.-G.; Hsieh-Li, H.-M.; Jong, Y.-J.; Wang, N. M.; Tsai, C.-H.; Li, H. Treatment of spinal muscular atrophy by sodium butyrate. *Proc. Natl. Acad. Sci. U.S.A.*, **2001**, *98*, 9808–9813.

<sup>xvi</sup> Andreassi, C.; Angelozzi, C.; Tiziano, F. D.; Vitali, T.; Vincenzi, E. D.; Boninsegna, A.; Villanova, M.; Bertini, E.; Pini, A.; Neri, G.; Brahe, C. Phenylbutyrate increases SMN expression *in vitro*: relevance for treatment of spinal muscular atrophy. *Eur. J. Hum. Genet.*, **2004**, *12*, 59–65.

<sup>xvii</sup> Grzeschik, S. M.; Ganta, M.; Prior, T. W.; Heavlin, W. D.; Wang, C. H. Hydroxyurea enhances *SMN2* gene expression in spinal muscular atrophy cells. *Ann. Neurol.*, **2005**, *58*, 194–202.

<sup>xviii</sup> Wirth, B.; Riessland, M.; Hahnen, E. Drug discovery for spinal muscular atrophy. *Expert Opin. Drug Discov.*, **2007**, *2*, 437-451.

<sup>xix</sup> (a) Brichta, L.; Hofmann, Y.; Hahnen, E.; Siebzehnruhl, F. A.; Raschke, H.; Blumcke, I.; Eyupoglu, I. Y.; Wirth, B. Valproic acid increases the *SMN2* protein level: a well-known drug as a potential therapy for spinal muscular atrophy. *Hum. Mol. Genet.*, **2003**, *12*, 2481–2489. 32. (b) Sumner, C. J.; Huynh, T. N.; Markowitz, J. A.; Perhac, J. S.; Hill, B.; Coover, D. D.; Schussler, K.; Chen, X.; Jarecki, J.; Burghes, A. H. M.; Taylor, J. P.; Fischbeck, K. H. Valproic acid increases SMN levels in spinal muscular atrophy patient cells. *Ann. Neurol.*, **2003**, *54*, 647-654.

<sup>xx</sup> Andreassi, C.; Jarecki, J.; Zhou, J.; Coover, D. D.; Monani, U. R.; Chen, X.; Whitney, M.; Pollok, B.; Zhang, M.; Androphy, E. J.; Burghes, A. H. M. Aclarubicin treatment restores SMN levels to cells derived from type I spinal muscular atrophy patients. *Hum. Mol. Genet.*, **2001**, *10*, 2841–2849.

<sup>xxi</sup> Wolstencroft, E. C.; Mattis, V.; Bajer, A. A.; Young, P. J.; Lorson, C. L. A non-sequence-specific requirement for SMN protein activity: the role of aminoglycosides in inducing elevated SMN protein levels. *Hum. Mol. Genet.*, **2005**, *14*, 1199-1210.

---

<sup>xxii</sup> Avila, A. M.; Burnett, B. G.; Taye, A. A.; Gabanella, F.; Knight, M. A.; Hartenstein, P.; Cizman, Z.; Di Prospero, N. A.; Pellizzoni, L.; Fischbeck, K. H.; Sumner, C. J. Trichostatin A increases SMN expression and survival in a mouse model of spinal muscular atrophy. *J. Clin. Invest.*, **2007**, *117*, 659-671.

<sup>xxiii</sup> (a) Hahnen, E.; Eyupoglu, I. Y.; Brichta, L.; Haastert, K.; Trankle, C.; Siebzebruhl, F. A.; Riessland, M.; Holker, I.; Claus, P.; Romstock, J.; et al. In vitro and ex vivo evaluation of second-generation histone deacetylase inhibitors for the treatment of spinal muscular atrophy. *J. Neurochem.*, **2006**, *98*, 193–202. (b) Riessland, M.; Ackermann, B.; Förster, A.; Jakubik, M.; Hauke, J.; Garbes, L.; Fritzsche, I.; Mende, Y.; Blumcke, I.; Hahnen, E.; Wirth, B. SAHA ameliorates the SMA phenotype in two mouse models for spinal muscular atrophy. *Hum. Mol. Genet.*, **2010**, *19*, 1492-1506.

<sup>xxiv</sup> Yuo, C.-Y.; Lin, H.-H.; Chang, Y.-S.; Yang, W.-K.; Chang, J.-G. 5-(*N*-ethyl-*N*-isopropyl)-amiloride enhances *SMN2* exon 7 inclusion and protein expression in spinal muscular atrophy cells. *Ann. Neurol.*, **2008**, *63*, 26–34.

<sup>xxv</sup> **Garbes, L.; Riessland, M.; Hölker, I.; Heller, R.; Hauke, J.; Tränkle, C.; Coras, R.; Blümcke, I.; Hahnen, E.; Wirth, B.** LBH589 induces up to 10-fold SMN protein levels by several independent mechanisms **and** is effective even in cells from SMA patients non-responsive to valproate. *Hum. Mol. Genet.*, **2009**, *18*, 3645-3658.

<sup>xxvi</sup> Dayangaç-Erden, D.; Bora, G.; Ayhan, P.; Kocafe, C.; Dalkara, S.; Yelekçi, K.; Demir, A. S. Erdem-Yurter, H. Histone deacetylase inhibition activity and molecular docking of (*E*)-Resveratrol: its therapeutic potential in spinal muscular atrophy. *Chem. Biol. Drug Design*, **2009**, *73*, 355-364.

<sup>xxvii</sup> Lunn, M. R.; Root, D. E.; Martino, A. M.; Flaherty, S. P.; Kelley, B. P.; Coover, D. D.; Burghes, A. H. M.; thi Man, N.; Morris, G. E.; Zhou, J.; Androphy, E. J.; Sumner, C. J.; Stockwell, B. R. Indoprofen upregulates the survival motor neuron protein through a cyclooxygenase-independent mechanism. *Chem. Biol.*, **2004**, *11*, 1489-1493.

<sup>xxviii</sup> Hastings, M. L.; Berniac, J.; Liu, Y. H.; Abato, P.; Jodelka, F. M.; Barthel, L.; Kumar, S.; Dudley, C.; Nelson, M.; Larson, K.; Edmonds, J.; Bowser, T.; Draper, M.; Higgins, P.; Krainer, A. R. Tetracyclines that promote *SMN2* exon 7 splicing as therapeutics for spinal muscular atrophy. *Sci. Transl. Med.*, **2009**, *1*, 5ra12.

<sup>xxix</sup> Jarecki, J.; Chen, X.; Bernardino, A.; Coover, D. D.; Whitney, M.; Burghes, A. H. M.; Stack, J.; Pollok, B. A. Diverse small-molecule modulators of SMN expression found by high-throughput compound screening: early leads towards a therapeutic for spinal muscular atrophy. *Hum. Mol. Genet.*, **2005**, *14*, 2003-2018.

<sup>xxx</sup> (a) Thurmond, J.; Butchbach, M. E.; Palomo, M.; Pease, B.; Rao, M.; Bedell, L.; Keyvan, M.; Pai, G.; Mishra, R.; Haraldsson, M.; Andresson, T.; Bragason, G.; Thosteinsdottir, M.; Bjornsson, J. M.; Coover, D. D.; Burghes, A. H. M.; Gurney, M. E.; Singh, J. Synthesis and biological evaluation of novel 2,4-diaminoquinazoline derivatives as *SMN2* promoter activators for the potential treatment of spinal

---

muscular atrophy. *J. Med. Chem.*, **2008**, *51*, 449-469. (b) Singh, J.; Salcius, M.; Liu, S. W.; Staker, B. L.; Mishra, R.; Thurmond, J.; Michaud, G.; Mattoon, D. R.; Printen, J.; Christensen, J.; Bjornsson, J. M.; Pollok, B. A.; Kiledjian, M.; Stewart, L.; Jarecki, J.; Gurney, M. E. DcpS as a therapeutic target for spinal muscular atrophy. *ACS Chem. Biol.*, **2008**, *3*, 711-722.

<sup>xxx</sup> Butchbach, M. E.; Singh, J.; Thornorsteinsdóttir, M.; Saieva, L.; Slominski, E.; Thurmond, J.; Andrésson, T.; Zhang, J.; Edwards, J. D.; Simard, L. R.; Pellizzoni, L.; Jarecki, J.; Burghes, A. H. M.; Gurney, M. E. Effects of 2,4-diaminoquinazoline derivatives on SMN expression and phenotype in a mouse model for spinal muscular atrophy. *Hum. Mol. Genet.*, **2009**, *19*, 454-467.

<sup>xxxii</sup> *Chemical & Engineering News*, April 26, **2010**.

<sup>xxxiii</sup> It is interesting to find that <sup>both</sup> D156844 and another analogue **5g** <sup>in reference 30a</sup> were not active in our <sup>current</sup> in-house luciferase reporter assay.

<sup>xxxiv</sup> Nicolaou, K. C.; He, Y.; Roschangar, F.; King, N. P.; Vourloumis, D.; Li, T. Total synthesis of epothilone E & analogs with modified side chains through the Stille coupling reaction. *Angew. Chem., Int. Ed. Engl.*, **1998**, *37*, 84-87.

<sup>xxxv</sup> Miyaura, N.; Suzuki, A. Palladium-catalyzed cross-coupling reactions of organoboron compounds. *Chem. Rev.*, **1995**, *95*, 2457-2483.

<sup>xxxvi</sup> Jolidon, S.; Narquizian, R.; Norcross, R. D.; Pinard, E. [4-(Heteroaryl) piperazin-1-yl]-(2,5-substituted-phenyl)methanone derivatives as glycine transporter 1 (glyt-1) inhibitors for the treatment of neurological and neuropsychiatric disorders. *PCT Patent Application: WO2006/72436 A1*, **2006**.

<sup>xxxvii</sup> Palani, A.; Berlin, M. Y.; Aslanian, R. G.; Vaccaro, H. M.; Chan, T.-Y.; Xiao, D.; Degrado, S.; Rao, A. U.; Chen, X.; Lee, Y. J.; Sofolarides, M. J.; Shao, N.; Huang, Y. R.; Liu, Z.; Wang, L. Y.; Pu, H. Pyrrolidine, piperidine and piperazine derivatives and methods of use thereof. *PCT Patent Application: WO2010/45303 A2*, **2010**.

<sup>xxxviii</sup> Plant, A.; Seitz, T.; Jansen, J. R.; Erdelen, C.; Turberg, A.; Hansen, O. Delta 1-pyrrolines used as pesticides. *U.S. Patent Application: US2004/82586 A1*, **2004**.

<sup>xxxix</sup> Sekiguchi, Y.; Kanuma, K.; Omodera, K.; Tran, T.-A.; Semple, G.; Kramer, B. A. Pyrimidine derivatives and methods of treatment related to the use thereof. *PCT Patent Application: WO/2005/095357*, **2005**.

<sup>xl</sup> Westhuyzen, C. W. van der; Rousseau, A. L.; Parkinson, C. J. Effect of substituent structure on pyrimidine electrophilic substitution. *Tetrahedron*, **2007**, *63*, 5394-5405.

<sup>xli</sup> Devasagayaraj, A.; Jin, H.; Liu, Q.; Marinelli, B.; Samala, L.; Shi, Z.-C.; Tunoori, A.; Wang, Y.; Wu, W.; Zhang, C.; Zhang, H. Multicyclic amino acid derivatives and methods of their use. *U.S. Patent Application: US2007/191370 A1*, **2007**.

---

<sup>xlii</sup> Zhang, M. L.; Lorson, C. L.; Androphy, E. J.; Zhou, J. An *in vivo* reporter system for measuring increased inclusion of exon 7 in *SMN2* mRNA: potential therapy of SMA. *Gene Therapy*, **2001**, *8*, 1532–1538.

<sup>xliii</sup> Inglese, J.; Auld, D. S.; Jadhav, A.; Johnson, R. L.; Simeonov, A.; Yasgar, A.; Zheng, W.; Austin, C. P. Quantitative high-throughput screening: A titration-based approach that efficiently identifies biological activities in large chemical libraries. *Proc. Natl. Acad. Sci. U.S.A.*, **2006**, *103*, 11473–11478.

<sup>xliv</sup> Austin, C. P.; Brady, L. S.; Insel, T. R.; Collins, F. S. NIH molecular libraries initiative. *Science* **2004**, *306*, 1138–1139.

<sup>xlv</sup> (a) Auld, D. S.; Zhang, Y. Q.; Southall, N. T.; Rai, G.; Landsman, M.; Maclure, J.; Langevin, D.; Thomas, C. J.; Austin, C. P.; Inglese, J. A basis for reduced chemical library inhibition of firefly luciferase obtained from directed evolution. *J. Med. Chem.*, **2009**, *52*, 1450–1458. (b) Auld, D. S.; Thorne, N.; Nguyen, D.-T.; Inglese, J. A specific mechanism for nonspecific activation in reporter-gene assays. *ACS Chem. Bio.*, **2008**, *3*, 463–470. (c) Auld, D. S.; Thorne, N.; Maguire, W. F.; Inglese, J. Mechanism of PTC124 activity in cell-based luciferase assays of nonsense codon suppression. *Proc. Natl. Acad. Sci. U.S.A.*, **2009**, *106*, 3585–3590.

<sup>xlvi</sup> Xia, M.; Huang, R.; Guo, V.; Southall, N.; Cho, M.-H.; Inglese, J.; Austin, C. P.; Nirenberg, M. Identification of compounds that potentiate CREB signaling as possible enhancers of long-term memory. *Proc. Natl. Acad. Sci. U.S.A.*, **2009**, *106*, 2412–2417.

<sup>xlvii</sup> van Breemen, R. B.; Li, Y. Caco-2 cell permeability assays to measure drug absorption. *Expert Opin. Drug Metab. Toxicol.*, **2005**, *1*, 175–185.

<sup>xlviii</sup> Aller, S. G.; Yu, J.; Ward, A.; Weng, Y.; Chittaboina, S.; Zhuo, R.; Harrell, P. M.; Trinh, Y. T.; Zhang, Q.; Urbatsch, I. L.; Chang, G. Structure of P-glycoprotein reveals a molecular basis for poly-specific drug binding. *Science*, **2009**, *323*, 1718–1722.

<sup>xlix</sup> Coover, D. D.; Le, T. T.; McAndrew, P. E.; Strasswimmer, J.; Crawford, T. O.; Mendell, J. R.; Coulson, S. E.; Androphy, E. J.; Prior, T. W.; Burghes, A. H. M. The survival motor neuron protein in spinal muscular atrophy. *Hum. Mol. Genet.* **1997**, *6*, 1205–1214.

<sup>1</sup> We have seen this pattern previously with LDDN hits (unpublished results from the laboratory of Elliot J. Androphy).